Molecular Plant
Research article

CellPress
Partner Journal

A circular single-stranded DNA mycovirus infects plants and confers broad-spectrum fungal resistance

Xianhong Wang[1,2,3,4], Ioly Kotta-Loizou[5,6], Robert H.A. Coutts[6], Huifang Deng[1,2,3,4], Zhenhao Han[1,2,3,4], Ni Hong[3,4], Karim Shafik[1,2,3,4,7], Liping Wang[1,3,4], Yashuang Guo[1,2,3,4], Mengmeng Yang[1,2,3,4], Wenxing Xu[1,2,3,4,*] and Guoping Wang[1,3,4,*]

[1]National Key Laboratory for Germplasm Innovation & Utilization of Horticultural Crops, Wuhan 430070, China

[2]Hubei Hongshan Laboratory, Wuhan 430070, China

[3]College of Plant Science and Technology, Huazhong Agricultural University, Wuhan 430070, China

[4]Key Lab of Plant Pathology of Hubei Province, Wuhan 430070, China

[5]Department of Life Sciences, Faculty of Natural Sciences, Imperial College London, London SW7 2AZ, UK

[6]Department of Clinical, Pharmaceutical and Biological Science, School of Life and Medical Sciences, University of Hertfordshire, Hatfield AL10 9AB, UK

[7]Department of Plant Pathology, Faculty of Agriculture, Alexandria University, Alexandria 21526, Egypt

***Correspondence: Wenxing Xu (xuwenxing@mail.hzau.edu.cn), Guoping Wang (gpwang@mail.hzau.edu.cn)**

https://doi.org/10.1016/j.molp.2024.05.003

ABSTRACT

Circular single-stranded DNA (ssDNA) viruses have been rarely found in fungi, and the evolutionary and ecological relationships among ssDNA viruses infecting fungi and other organisms remain unclear. In this study, a novel circular ssDNA virus, tentatively named Diaporthe sojae circular DNA virus 1 (DsCDV1), was identified in the phytopathogenic fungus *Diaporthe sojae* isolated from pear trees. DsCDV1 has a monopartite genome (3185 nt in size) encapsidated in isometric virions (21–26 nm in diameter). The genome comprises seven putative open reading frames encoding a discrete replicase (Rep) split by an intergenic region, a putative capsid protein (CP), several proteins of unknown function (P1–P4), and a long intergenic region. Notably, the two split parts of DsCDV1 Rep share high identities with the Reps of *Geminiviridae* and *Genomoviridae*, respectively, indicating an evolutionary linkage with both families. Phylogenetic analysis based on Rep or CP sequences placed DsCDV1 in a unique cluster, supporting the establishment of a new family, tentatively named *Gegemycoviridae*, intermediate to both families. DsCDV1 significantly attenuates fungal growth and nearly erases fungal virulence when transfected into the host fungus. Remarkably, DsCDV1 can systematically infect tobacco and pear seedlings, providing broad-spectrum resistance to fungal diseases. Subcellular localization analysis revealed that DsCDV1 P3 is systematically localized in the plasmodesmata, while its expression in *trans*-complementation experiments could restore systematic infection of a movement-deficient plant virus, suggesting that P3 is a movement protein. DsCDV1 exhibits unique molecular and biological traits not observed in other ssDNA viruses, serving as a link between fungal and plant ssDNA viruses and presenting an evolutionary connection between ssDNA viruses and fungi. These findings contribute to expanding our understanding of ssDNA virus diversity and evolution, offering potential biocontrol applications for managing crucial plant diseases.

Key words: circular single-stranded DNA virus, mycovirus, virus evolution, *Genomoviridae*, *Gegemycoviridae*, Diaporthe sojae circular DNA virus 1

Wang X., Kotta-Loizou I., Coutts R.H.A., Deng H., Han Z., Hong N., Shafik K., Wang L., Guo Y., Yang M., Xu W., and Wang G. (2024). A circular single-stranded DNA mycovirus infects plants and confers broad-spectrum fungal resistance. Mol. Plant. **17**, 955–971.

Published by the Molecular Plant Shanghai Editorial Office in association with Cell Press, an imprint of Elsevier Inc., on behalf of CSPB and CEMPS, CAS.

INTRODUCTION

Circular replicase-encoding single-stranded (CRESS) DNA viruses have been reported to infect almost all living organisms (Krupovic, 2013; Zhao et al., 2019). Since single-stranded DNA (ssDNA) viruses are highly diverged, representing polyphyletic groups that can infect organisms across all three life domains (archaea, bacteria, and eukarya), their origin and evolution remain poorly understood, with a few exceptions: for instance, geminiviral replicase (Rep) proteins share a common ancestral origin with those of phytoplasma plasmids (Kazlauskas et al., 2019; Anirudha and Bikash, 2020).

According to the International Committee on the Taxonomy of Viruses (http://ictv.global/report), CRESS DNA viruses are currently classified into 11 families. Among them, the members of seven families (*Anelloviridae*, *Bacilladnaviridae*, *Circoviridae*, *Geminiviridae*, *Genomoviridae*, *Nanoviridae*, and *Smacoviridae*) infect eukaryotic organisms. Members of families *Geminiviridae* and *Nanoviridae* infect plants as important phytopathogens, posing a great threat to global agriculture and food security (Scholthof et al., 2011). Both families are responsible for considerable losses in economically important crops, including tomato, maize, wheat, sugar cane, cassava, cucurbits, sweet potatoes, pepper, and cotton (Rojas et al., 2018; García-Arenal and Zerbini, 2019; Lal et al., 2020), and induce a range of symptoms in their plant hosts, including stunting, dwarfing, necrosis, mosaic, leaf rolling, and even plant death (Rojas et al., 2018; Lal et al., 2020; Li et al., 2022).

Unlike plant CRESS DNA viruses, which are commonplace worldwide and include >500 species belonging to *Geminiviridae* and *Nanoviridae*, fungal CRESS DNA viruses have been rarely identified and characterized. Only Sclerotinia sclerotiorum hypovirulence-associated DNA virus 1 (SsHADV-1) and Fusarium graminearum gemytripvirus 1 (FgGMTV1) have been accepted as members belonging to two different genera of the family *Genomoviridae* (Varsani and Krupovic, 2021), which accommodates geminivirus-like mycoviruses without a movement protein (MP) and is well characterized (Yu et al., 2010; Krupovic et al., 2016; Li et al., 2020).

In the field, fungi can colonize plants, establishing complex endophytic, parasitic, or mycorrhizal relationships and allowing interactions between plant and fungal viruses (Priyashantha et al., 2023). Therefore, many viral families include members that infect both plants and fungi with suspected evolutionary links (Roossinck, 2018). However, except for the traits of a circular ssDNA genome and the conserved motifs in Rep, viruses in the family *Genomoviridae* share no detectable similarities in their Rep or capsid protein (CP) sequences with viruses infecting plants and other organisms. Therefore, evolutionary and ecological relationships among ssDNA viruses infecting fungi and other organisms are poorly understood.

Mycoviruses (fungal viruses) were discovered much later than viruses that infect plants, animals, and bacteria (Ghabrial et al., 2015; Son et al., 2015). Over the last decade, reports on the occurrence and complete genetic characterization of mycoviruses have escalated exponentially mainly through technological advances, particularly next-generation sequencing (NGS). These investigations have broadened our knowledge on mycovirus diversity and evolution (Marzano et al., 2016; Hillman et al., 2018; Mu et al., 2018; Zhong et al., 2022). NGS has demonstrated that the mycovirome consist mainly of viruses with positive-sense ssRNA (+ssRNA) and double-stranded RNA (dsRNA) genomes; however, smaller numbers of both negative-sense ssRNA (−ssRNA) and ssDNA genomes have also been described (Yu et al., 2010; Li et al., 2020; Kondo et al., 2022; Raco et al., 2022; Wang et al., 2022). The first ssDNA mycovirus, SsHADV-1, was isolated from the phytopathogenic fungus *Sclerotinia sclerotiorum* in 2010 (Yu et al., 2010), followed by FgGMTV1, which was isolated from *Fusarium graminearum* in 2020 (Li et al., 2020), together with Botrytis cinerea ssDNA virus 1 (BcssDV1) (Ruiz-Padilla et al., 2021, 2023) and Botrytis cinerea gemydayirivirus 1 (BcGDV1) (Khalifa and MacDiarmid, 2021), which were isolated from *Botrytis cinerea*. Recently, several sequences related to genomoviruses have been detected in various organisms, including plants (Dayaram et al., 2012; Kraberger et al., 2015; Nery et al., 2023), humans (Halary et al., 2016), animals (Li et al., 2015; Schmidlin et al., 2019), and environmental samples (Kraberger et al., 2021), suggesting that CRESS DNA viruses infecting fungi potentially have an evolutionary link and are closely related to those infecting other organisms. Moreover, the biological traits of CRESS DNA mycoviruses are well characterized, and they have been reported to dramatically modulate the virulence of their hosts (Yu et al., 2010, 2013; Xie and Jiang, 2014; Qu et al., 2020; Zhang et al., 2023). For example, SsHADV-1 was shown to significantly suppress *S. sclerotiorum* infection in oilseed rape plants (Yu et al., 2010, 2013; Xie and Jiang, 2014; Qu et al., 2020), converting the phytopathogenic lifestyle of the fungus to a beneficial endophytic lifestyle that improves crop health and yield. Additionally, this study reports successful application of a mycovirus as a biocontrol agent to control fungal disease in the field (Tian et al., 2020; Zhang et al., 2020). Similar control methods were employed previously with Cryphonectria hypovirus 1 (CHV-1), which was applied on chestnut trees to control chestnut blight caused by the phytopathogenic fungus *Cryphonectria parasitica* in Europe (Anagnostakis, 1982; Heiniger and Rigling, 1994). Moreover, FgGMTV1, which is a tripartite CRESS DNA mycovirus, was successfully used to construct a virus-induced gene silencing (VIGS) vector to silence virulence genes related to *Fusarium* spp. head blight disease in cereals. The VIGS vector converted the virulent *F. graminearum* strain tested into a hypovirulent strain, leading to successful disease control in wheat (Zhang et al., 2023). However, the molecular mechanisms of how ssDNA mycoviruses alter fungal virulence are as yet unknown and much investigation is still required.

Diaporthe (the sexual morph of *Phomopsis*) spp. are widely distributed, causing severe diseases with significant losses in a wide range of plants including fruit trees, forest trees, vegetables, and ornamental plants (Santos et al., 2011; Thompson et al., 2011; Guarnaccia et al., 2018; Zhao et al., 2022). In pear trees, *Diaporthe* spp. cause brown canker symptoms around the buds, ultimately leading to the death of the infected shoots, twigs, or branches in severe situations (Guo et al., 2020). In our previous studies, 19 *Diaporthe* species were identified as being responsible for shoot canker symptoms on pear trees, including *Pyrus bretschneideri*, *P. communis*, *P. pyrifolia*, and *P. ussuriensis*, grown in 12 different Chinese provinces (Bai et al., 2015; Guo et al., 2020).

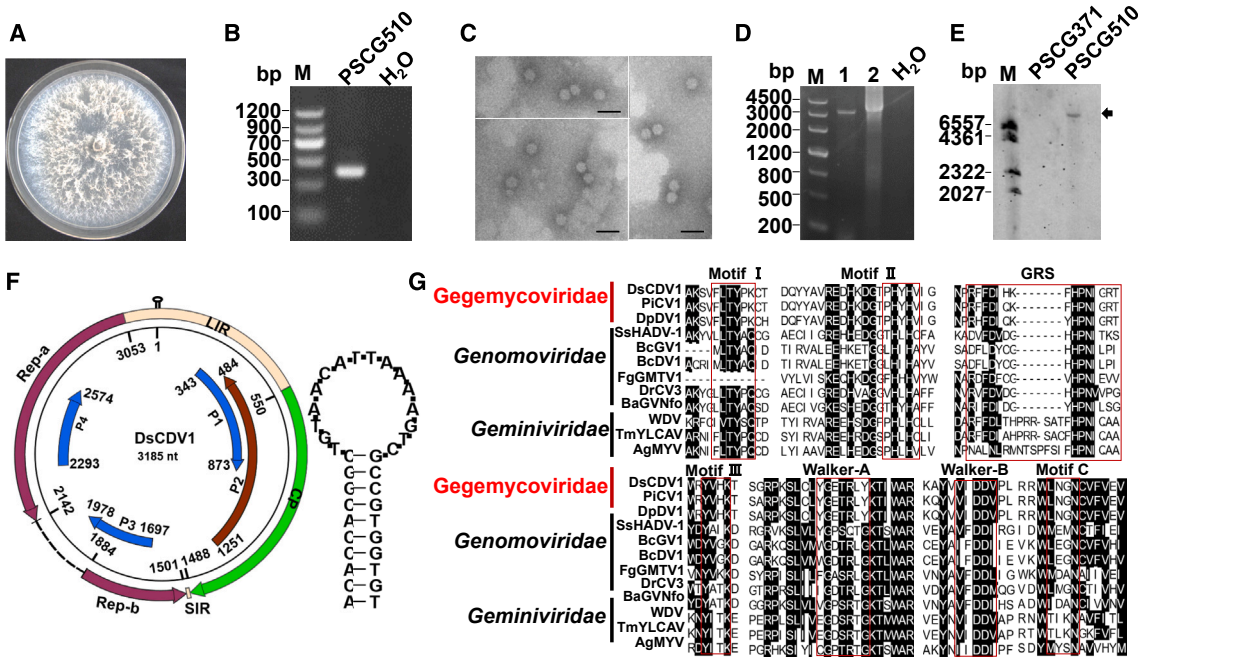

Figure 1. Characterization of Diaporthe sojae circular DNA virus 1 (DsCDV1) infecting *Diaporthe sojae* strain PSCG510.
(A) Colony morphology of *D. sojae* strain PSCG510 cultured on PDA in darkness 5 days post inoculation (dpi).
(B) Agarose gel electrophoresis of PCR amplicons of DsCDV1 in *D. sojae* strain PSCG510. Lane M: DNA marker.
(C) Viral particles purified from PSCG510 mycelia as visualized by TEM. Scale bars, 50 nm.
(D) Agarose gel electrophoresis of PCR amplicons diagnostic for DsCDV1. RCA products of DsCDV1 after enzymatic treatment with *Sac*I (lane 1) and PCR amplicons produced with abutted primers (DsCDV1-All-F/-R, lane 2) for DsCDV1 detection in PSCG510.
(E) Southern blotting analysis of DsCDV1 in PSCG510, with strain PSCG371 used as a negative control. M, digoxin-labeling DNA marker. The signal corresponding toDsCDV1 is indicated by an arrow.
(F) Genome organization of DsCDV1 (left) and the stem-loop secondary structure of the partial large intergenic region around the nona-nucleotide sequence (right).
(G) Multiple alignments of the Rep conserved domains of DsCDV1 and selected members belonging to the families *Genomoviridae* and *Geminiviridae*.

Management of pear shoot canker mainly relies on chemical fungicides. However, global concerns about food safety have stimulated our investigation to identify hypovirulence-related ssDNA mycoviruses to attenuate fungal virulence and control disease.

In this study, a novel CRESS DNA mycovirus was identified and characterized in a phytopathogenic fungus isolated from pear trees. This mycovirus possesses a hybrid Rep gene related to both fungal and plant CRESS DNA viruses and can infect both fungi and plants, attenuating the virulence of the fungal host and conferring plant resistance against a wide range of phytopathogenic fungi. With unique molecular and biological traits not previously encountered in other ssDNA viruses, this mycovirus may represent a new family, providing an evolutionary and ecological link between fungal and plant CRESS DNA viruses as well as a potential biocontrol agent for managing fungal diseases in pear trees.

RESULTS

High-throughput sequencing reveals two contigs related to an ssDNA virus infecting *Diaporthe* spp

To investigate ssDNA virus(es) infecting *Diaporthe* fungi, 80 strains of 10 *Diaporthe* species (*D. caryae*, *D. citrichinensis*, *D. eres*, *D. fusicola*, *D. hongkongensis*, *D. padina*, *D. sojae*, *D. taoicola*, *D. unshiuensis*, and *D. velutina*) were isolated from pear plants (*Pyrus bretschneideri*, *P. communis*, and *P. pyrifolia*) showing shoot canker symptoms collected from 10 provinces (Fujian, Guizhou, Henan, Hubei, Jiangsu, Jiangxi, Liaoning, Shandong, Yunnan, and Zhejiang) and Chongqing municipality, China (Supplemental Table 1), and grown on potato dextrose agar (PDA). Following high-throughput sequencing (HTS) targeting RNAs lacking a poly(A) tail of eight cohorts containing 10 strains each, a total of 66 276 874 reads were obtained and assembled into 650 360 contigs. Of these, only one cohort of eight stains processed together had two contigs, respectively 1230 and 1144 bp in size (Supplemental data 1), which were shown by the Basic Local Alignment Search Tool (BLAST)x to be related to ssDNA viruses.

Determination of the genomic sequence of ssDNA virus and visualization of its particles

To identify the exact strain(s) infected with the putative ssDNA virus, the eight strains in the virus-related cohort were cultured and subjected to DNA extraction. PCR amplification was used to identify the virus using a pair of specific primers (contig_31484F/-R, Supplemental Table 2), which were designed based on the contig sequences. Following agarose gel fractionation, a DNA band with the expected size of 406 bp (Figure 1A and 1B) was obtained from *D. sojae* strain PSCG510 isolated from Jiangsu province, China. To obtain the complete genome of the ssDNA

virus, DNA extracted from PSCG510 was amplified by PCR using a pair of abutted primers (DsCDV1-All-F/-R, Supplemental Table 2). After DNA purification, cloning, and sequencing, the full genome of the ssDNA virus, 3185 nt in size, was obtained. This was further confirmed by rolling circle amplification (RCA) followed by restriction digestion with *Sac*I: a single DNA band of ~3.2 kbp in size was obtained (Figure 1D, lane 1), which matched in size the amplicon identified by PCR using the pair of abutted primers (Figure 1D, lane 2). The circular nature of the DNAs in strain PSCG510 was further examined by Southern blotting analysis with a digoxin-labeled probe, indicating that they migrate slower than the largest-sized double-stranded DNA marker, which has a size of 6557 bp (Figure 1E), and therefore are likely supercoiled. This virus was tentatively named Diaporthe sojae circular DNA virus 1 (DsCDV1). The full genomic sequence has been deposited in the GenBank database at the National Center for Biotechnology Information (NCBI) under the accession number GenBank: PP056609. According to BLASTn, DsCDV1 exhibits identities of 96.03% and 76.84% with those of Phomopsis longicolla circular virus 1 (PiCV1, KR106588; 99% coverage, *E* value = 0) and Diaporthe pseudophoenicicola DNA virus 1 (DpDV1, MW874642; 62% coverage, *E* value = 2e−160), respectively. Both PiCV1 and DpDV1 are yet to be characterized. However, no detectable identities were found with other viruses apart from a 71.26% identity with a partial region of tick-associated circular DNA virus (TaCV; 5% coverage, *E* value = 6e−11). It is worth noting that the DsCDV1 genome shares a 67.69% identity with the partial chromosome sequence of the medically important fungus *Cordyceps militaris* (CP023326; 9% coverage, *E* value = 7e−16).

To isolate DsCDV1 particles, PSCG510 mycelia were subjected to virion purification using sucrose density gradient ultracentrifugation (10–40% [w/v], with increments of 10%). Transmission electron microscopy (TEM) revealed isometric particles with a diameter of 21–26 nm in the 10%–20% sucrose fractions (Figure 1C).

To investigate the incidence of DsCDV1 in China, 453 strains of *Diaporthe* spp. were isolated from *Pyrus* branches (including *P. bretschneideri*, *P. communis*, *P. pyrifolia*, and *P. ussuriensis*) collected from 12 provinces in China (Guo et al., 2020) and subjected to PCR amplification using a pair of specific primers DsCDV1-F/-R (Supplemental Table 2). Expected DNA bands 552 bp in size were detected in 11 strains of four *Diaporthe* spp. (*D. eres*, *D. hongkongensis*, *D. fusicola*, and *D. sojae*) collected from five provinces (Hubei, Yunnan, Zhejiang, Guizhou, and Jiangsu) (Supplemental Figure 1 and Supplemental Table 3), suggesting that DsCDV1 has a low incidence (approximately 2.6%) in Chinese fields. Of these, three strains were sequenced following PCR amplification and aligned with the DsCDV1 sequence obtained from PSCG510. The results revealed over 99% similarity (Supplemental Table 4), indicating that DsCDV1 genomic sequences are highly conserved.

Molecular characterization and phylogenetic analysis of DsCDV1 reveals that it belongs to a new viral family

The DsCDV1 genome contains seven putative open reading frames (ORFs) >10 kDa, according to ORFfinder, with four ORFs located on the virion sense and the remaining three on the complementary sense (Figure 1F). The two major ORFs on the complementary-sense sequence are separated by an intergenic region (257 nt in size) and encode a fused Rep protein with a molecular mass (M_r) of 49.7 kDa. The third major putative ORF is located in the opposite orientation of the Rep-coding ORFs and encodes a putative CP (M_r 34.5 kDa). Between the Rep and CP coding ORFs, there is a large inverted repeat (IR) (681 nt in size) connecting the start codons of both ORFs, as well as a small IR (12 nt in size) connecting their stop codons. A nona-nucleotide sequence (TAACATTAA) is found within the large IR and likely acts as the initiation site for viral DNA replication (Figure 1F).

Multiple alignments of the Rep sequences of DsCDV1, along with other members belonging to the families *Genomoviridae* and *Geminiviridae*, revealed that the Rep sequence of DsCDV1 shares seven conserved motifs with those of genomoviruses and geminiviruses, including rolling circle replication (RCR) motifs (I, II, and III), helicase motifs (Walker-A, Walker-B, and motif C), and a geminivirus Rep sequence motif (Figure 1G). However, the Rep sequence of DsCDV1 has some unique amino acids including "uuTYxK" and "GxxxxYKT," observed in RCR motif I and helicase motif Walker-A, instead of "uuTYxQ" and "GxxxxGKT," respectively in the corresponding motifs of genomoviruses and geminiviruses (Figure 1G and Supplemental Table 5).

BLASTp revealed that the full sequence of Rep shares the highest sequence identity of 89.72% and 79.21% with those of the undetermined PiCV1 (AMN09328; 100% coverage, *E* value = 0) and DpDV1 (QVH35918; 100% coverage, *E* value = 0), respectively. Moreover, it shares low identities (ranging from 30.20% to 31.65%, 67%–68% coverage, *E* value = 5e−32 to e−26) with partially characterized genomoviruses found in plants and animals, e.g., Zizania latifolia genomovirus and Red panda feces-associated genomovirus, and 30.03% identity with a plant geminivirus, Melon chlorotic mosaic virus (MeCMV; 67% coverage, *E* value = 4e−29). It is worth noting that the Rep sequence of DsCDV1 shares considerably high identities (ranging from 28.48% to 56.16%, 40%–68% coverage, *E* value = 5e−76 to 1e−30) with the genomic sequences of some fungi, including *Xylaria arbuscula*, *Trichoglossum hirsutum*, *Russula earlei*, *Serpula lacrymans*, and *Amanita brunnescens* (Supplemental Table 6).

Moreover, BLASTp analysis of the N-terminal domain of DsCDV1 Rep located upstream the intergenic region (termed Rep-a) indicates that it shares high identities with genomic sequences of *X. arbuscula* and *T. hirsutum* (55% and 61% identities, 56.16% and 49.70% coverage, *E* value = 4e−78 and 1e−55, respectively) and the Reps of *Geminiviridae* members (60%–64% identities, 30.18%–35.03% coverage, *E* value = 4e−23 to 3e−21). Conversely, the C-terminal domain of DsCDV1 Rep located downstream of the intergenic region (termed Rep-b) shares high identities with genomic sequences of *R. earlei*, *S. lacrymans*, and *A. brunnescens* (77%–97% identities, 35.48%–41.84% coverage, *E* value = 9e−19 to 1e−16, respectively) and the Reps of *Genomoviridae* members (70%–80% identities, 40.38%–47.19% coverage, *E* value = 7e−16 to 2e−12) (Figure 2A). These results suggest that DsCDV1 Rep is a chimeric protein with different origins.

BLASTp showed that DsCDV1 CP shares high identities of 83.33% and 67.61% with PiCV1 (AMN09329; 100% coverage, *E* value = 0) and DpDV1 (QVH35917; 100% coverage, *E* value = 2e−144),

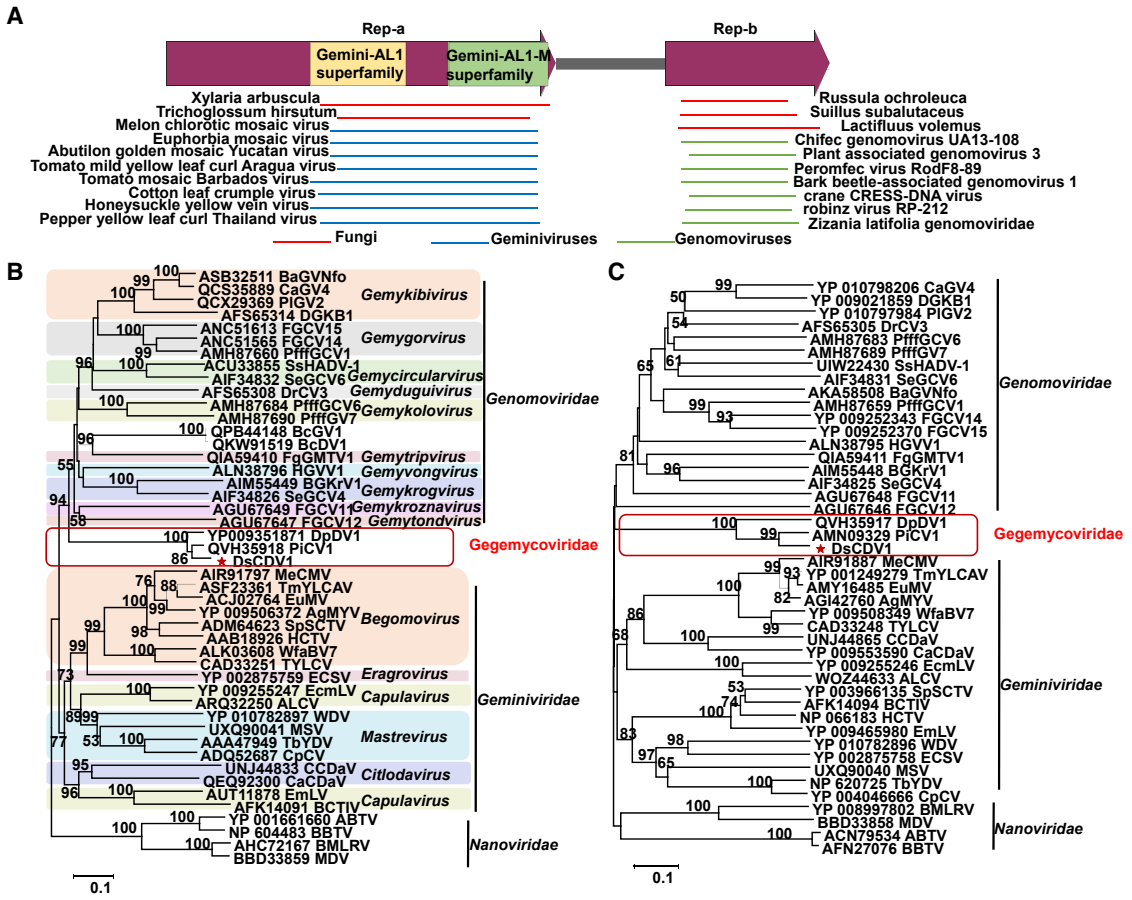

Figure 2. Phylogenetic analysis of DsCDV1.

(A) BLASTp hits of DsCDV1 Rep (separated into parts Rep-a and Rep-b) with related fungal genomic regions and Reps of genomoviruses and geminiviruses. Hits of fungi, genomoviruses, and geminiviruses are labeled in red, blue, and green, respectively.

(B and C) Phylogenetic analysis of DsCDV1 and closely related members selected from each genus of the families *Genomoviridae* and *Geminiviridae*. Phylogenetic trees were constructed based on Rep **(B)** and CP sequences **(C)** using the maximum-likelihood method as implemented by MEGA7. Numbers at the nodes indicate bootstrap values out of 1000 replicates (only values >50 are shown). The position of DsCDV1 is marked with a red star.

respectively, while no detectable identities with other viral proteins were detected. Moreover, it shares a 44% identity (27.88% coverage, *E* value = 0.003) with genomic sequences of the fungus *Xylaria nigripes*.

Phylogenetic trees were constructed based on the Rep (Figure 2B and Supplemental Figure 2A) and CP (Figure 2C and Supplemental Figure 2B) sequences of DsCDV1 together with some other representative members belonging to different genera of the families *Genomoviridae* and *Geminiviridae*, as well as some members belonging to the family *Nanoviridae* (Supplemental Table 7) . In both cases, the results showed that DsCDV1 is separated, together with PiCV1 and DpDV1, in a unique cluster, supporting the notion that they belong to a new family, tentatively named *Gegemycoviridae* (i.e., genomovirus- and geminivirus-like mycoviruses) and accommodating the proposed genus *Gegemycovirus*.

DsCDV1 alters morphology and attenuates the growth and virulence of host fungus

To investigate the biological traits of DsCDV1, attempts were made to obtain a DsCDV1-free isogenic line by single conidia isolation. Sporulation was induced in strain PSCG510 using several approaches as previously described (Guo et al., 2020), but without success. Due to the unavailability of conidia, we attempted to eliminate DsCDV1 from the hyphae of infected strain, but subculturing 48 cultures of strain PSCG510 every 3 days for 10 times using hyphal tips 3–5 mm long failed to eliminate DsCDV1 (Supplemental Figure 3A). Attempts to eliminate DsCDV1 from 48 or 24 cultures of strain PSCG510 following treatment with 50 μg/ml cycloheximide or ribavirin, respectively, also failed (Supplemental Figure 3B and 3C). Furthermore, all 108 subisolates of strain PSCG510 derived from single protoplast cells were found to be infected with DsCDV1 (Supplemental Figure 3D). These results indicate that DsCDV1 is difficult to eliminate, and a different approach was adopted to generate DsCDV1-infected and -free isogenic lines for phenotypic comparisons.

To infect other *D. fusicola* strains with DsCDV1, a 1.5-mer tandem repeat of DsCDV1 (pSK-1.5merDsCDV1) was constructed (Figure 3A), following a similar strategy previously reported for constructing infectious clones of geminiviruses (Saad et al., 2021). The construct was then transfected into protoplasts of

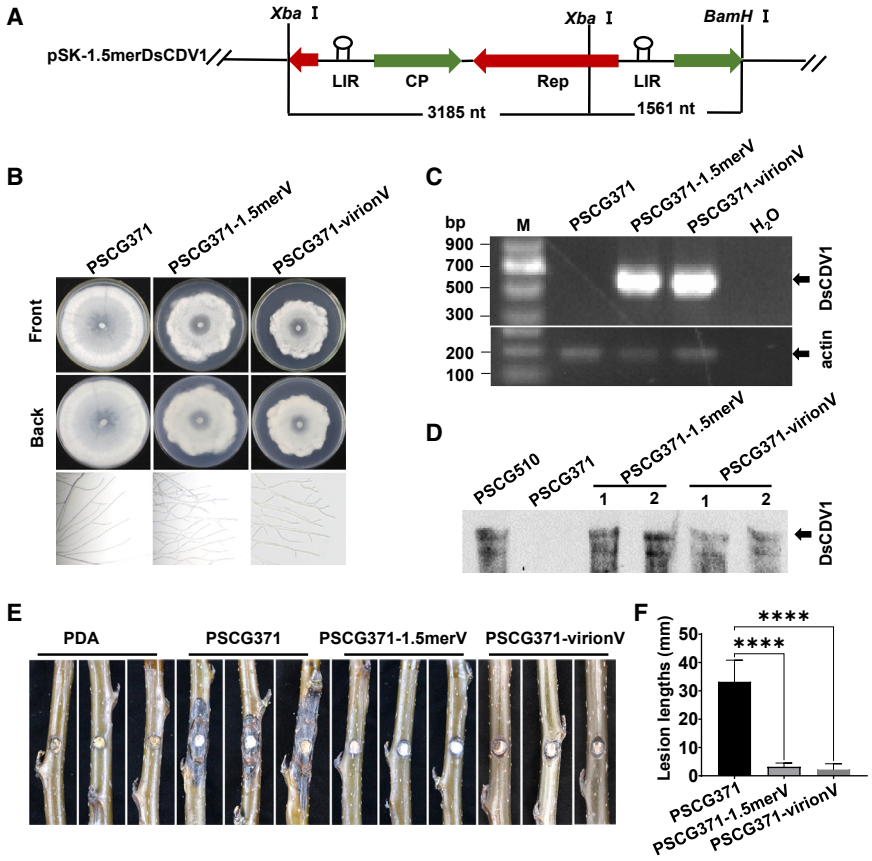

Figure 3. Effects of DsCDV1 on fungal morphology, growth, and virulence.

(A) Schematic diagram of construction of the infectious clone pSK-1.5merDsCDV1.

(B) Colony morphologies of PSCG371 and its transfectants (PSCG371-1.5merV and -virionV; subisolates of PSCG371 transfected with an infectious clone and purified virions of DsCDV1, respectively) cultured on PDA in darkness at 4 dpi.

(C and D) PCR **(C)** and Southern blot **(D)** detection of DsCDV1 in PSCG371 and its transfectants.

(E and F) Representative symptoms **(E)** and bar graph of lesion size **(F)** developed on pear shoots (*P. pyrifolia* cv. Cuiguan) following inoculation with PSCG371 and its transfectants at 7 dpi. Asterisks indicate significant differences ($p < 0.05$).

D. fusicola strain PSCG371, which was free of DsCDV1. Purified DsCDV1 particles were also transfected into protoplasts of the same strain. After transfection, the protoplasts were cultured on PDA, and the generated colonies were separately subjected to DNA extraction and PCR identification using primers DsCDV1-F/-R. The results revealed that 3 out of 45 colonies (6.67%) and 6 out of 96 colonies (6.25%) were positive for DsCDV1 infection after being transfected with pSK-1.5merDsCDV1 (termed strain PSCG371-1.5merV) and viral particles (termed PSCG371-virionV), respectively. These transfectants were serially subcultured for nine generations and subjected to identification of DsCDV1 infection by PCR (Figure 3C) and Southern blot (Figure 3D), indicating that DsCDV1 was stably detected in the fungal host. DsCDV1 infection in a representative transfectant was further confirmed through virion extraction and TEM visualization. The results showed that the viral particles recovered from PSCG371-virionV have a shape identical to those previously purified from parent strain PSCG510 (Supplemental Figure 4A).

Transfectants (PSCG371-1.5merV and PSCG371-virionV), together with their parent strain (PSCG371), were separately cultured on PDA to study the effect of DsCDV1 on their morphology and growth. Both transfectants exhibited abnormal morphology and significantly reduced growth rate (7 or 6 mm/day) as compared to their parent strain (10 mm/day). Moreover, the hyphal tips of both transfectants were swollen and dense, with much shorter branches (Figure 3B). The virulence of both transfectants and their parent strain was assessed on tender pear shoots (*P. pyrifolia* var. Cuiguan). Both transfectants induced significantly smaller lesions (2–3 mm) than those induced by their parent strain (33 mm) (Figure 3E and 3F). These results suggest that DsCDV1 significantly attenuates mycelial growth and virulence of the host fungus.

DsCDV1 is capable of transmission to other fungal species and systemic infection of plants

To investigate the horizontal transmissibility of DsCDV1 between *Diaporthe* strains, DsCDV1-infected strain PSCG510 as the donor was co-cultured pairwise with 13 DsCDV1-free strains belonging to 10 *Diaporthe* species (Supplemental Table 8) as recipients. Three mycelial disks, located far from the donor colonies, were excised from each recipient, subcultured for at least five generations, and subjected to PCR to assess DsCDV1 infection status. All subcultures of six strains from five species (*D. sojae*, *D. unshiuensis*, *D. taoicola*, *D. hongkongensis*, and *D. fusicola*) were infected with DsCDV1 (Supplemental Figure 3E). These results indicate that DsCDV1 can be efficiently transmitted to certain other *Diaporthe* strains or species through hyphal anastomosis.

To investigate whether DsCDV1, which is phylogenetically related to the plant geminivirus MeCMV, infects plants, basal leaves of pear seedlings (*P. betulaefolia*) were inoculated with mycelial plugs of strain PSCG510. At 20 days post inoculation (dpi), newly developed apical leaves of 20 seedlings were collected and subjected to PCR for DsCDV1 detection using primers DsCDV1-F/R. Six apical leaf samples tested positive for DsCDV1 infection (Figure 4A and 4B). To exclude the possibility of new leaves testing positive for DsCDV1 infection due to contamination by *D. sojae* strain PSCG510, the basal leaves used for inoculation and the apical leaves were separately collected, cut into small disks, and incubated on PDA to promote growth of fungi potentially present. As expected, fungal growth was observed at 3 dpi on PDA inoculated with basal leaf disks, but not apical leaf disks (Supplemental Figure 5A). All leaf disks were then subjected to nucleic acid extraction and PCR amplification with primer pairs ITS1/ITS4 (targeting partial regions of both plant and fungal internal transcribed spacers [ITS], resulting in

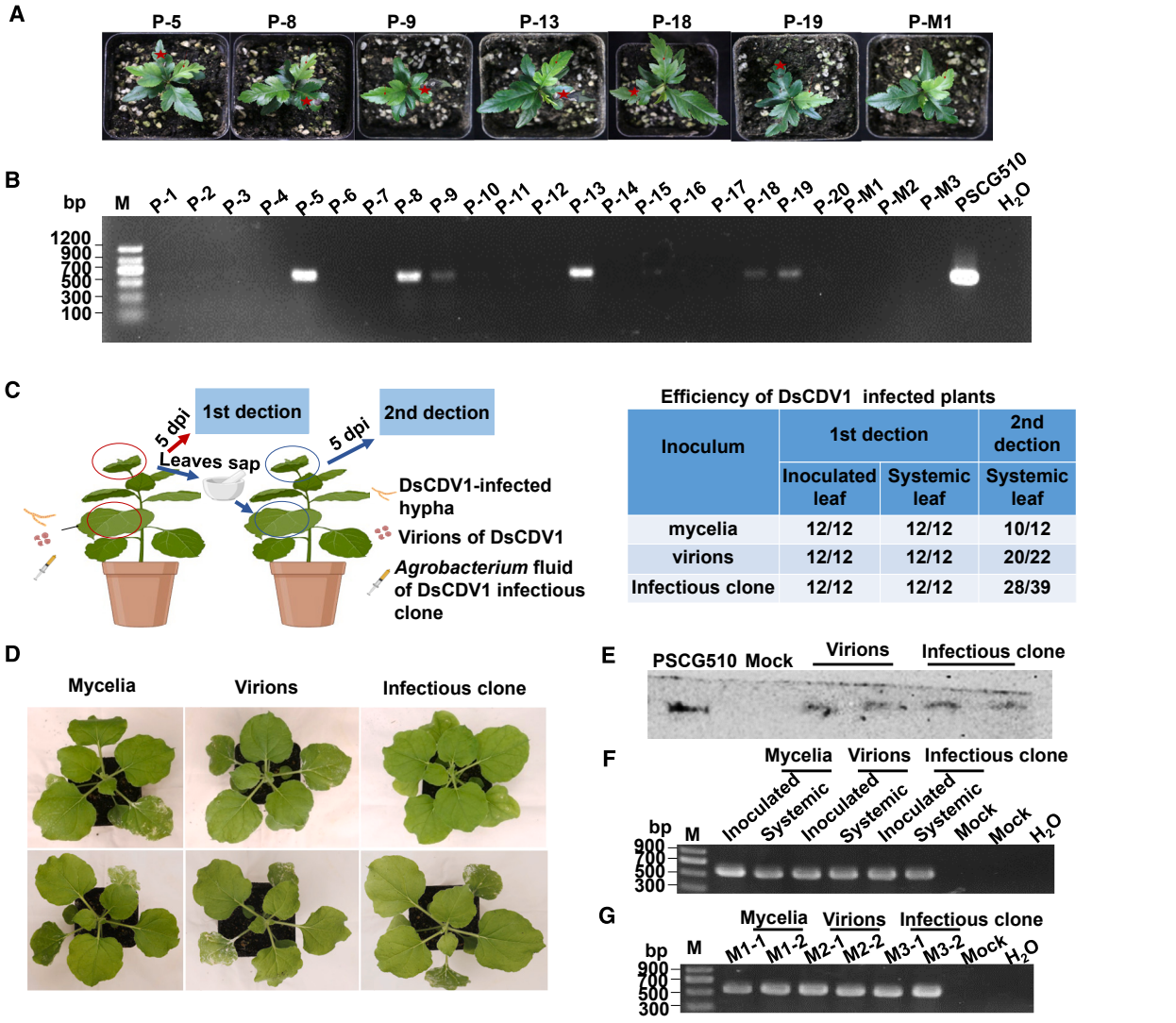

Figure 4. Infectivity of DsCDV1 in pear and tobacco plants.

(A and B) Representative phenotypes of the pear seedlings (*P. betulaefolia*) used for mechanical inoculation of DsCDV1 with mycelial plugs of strain PSCG510 **(A)**, and PCR detection of DsCDV1 in the inoculated seedlings 20 dpi **(B)**. The leaves used for inoculation and detection are marked with red stars and arrows, respectively. P-1 to P-20 refer to 20 seedlings inoculated with PSCG510 mycelial plugs, while PM1 to PM3 refer to seedlings treated with PDA disks.

(C) Schematic diagram of horizontal transmission of DsCDV1 into *N. benthamiana* plants after inoculation with fungal mycelia, virions, or infectious clones (left panel) and summary table of the positive rates revealed by PCR detection of DsCDV1 in the inoculated seedlings (right panel).

(D) Phenotypes of seedlings inoculated with fungal mycelia, virions, or infectious clones (upper panel) and their corresponding sap-transmitted seedlings (lower panel).

(E–G) Southern blot **(E)** and PCR detection **(F)** of DsCDV1 following inoculation with fungal mycelia, virions, or infectious clones and their corresponding sap-transmitted seedlings at 5 dpi **(G)**, in both basal leaves used for inoculation (lane 1) and newly developed apical leaves (lane 2).

amplicons respectively 682 and 570 bp in size) and U1/U2 (targeting a specific region of 28 rRNA of *D. sojae*, resulting in an amplicon 242 bp in size) (Supplemental Table 2). The targets for *D. sojae* ITS and 28 rRNA were amplified from basal leaves, while only plant ITS was amplified from apical leaves (Supplemental Figure 5B and 5C). These results confirm that DsCDV1 independently infects pear seedlings rather than being carried by the fungus as a vector for virus transmission.

The ability of DsCDV1 to infect plants in the absence of *D. sojae* was confirmed following mechanical inoculation of *Nicotiana benthamiana* leaves separately with purified viral particles and an infectious clone (pCB-1.5merDsCDV1) of DsCDV1, using mycelial disks of strain PSCG510 as a positive control in parallel. The leaves of inoculated plants were collected at 5 dpi and subjected to PCR and Southern blot for DsCDV1 detection. DsCDV1 was successfully detected in both basal and apical leaves of all 12 seedlings tested, previously inoculated with PSCG510 mycelia, viral particles, or an infectious clone, with no infection in control uninoculated seedlings (Figure 4C and 4G). Furthermore, apical leaves were collected from the *N. benthamiana* seedlings inoculated with the infectious clone and subjected to virion

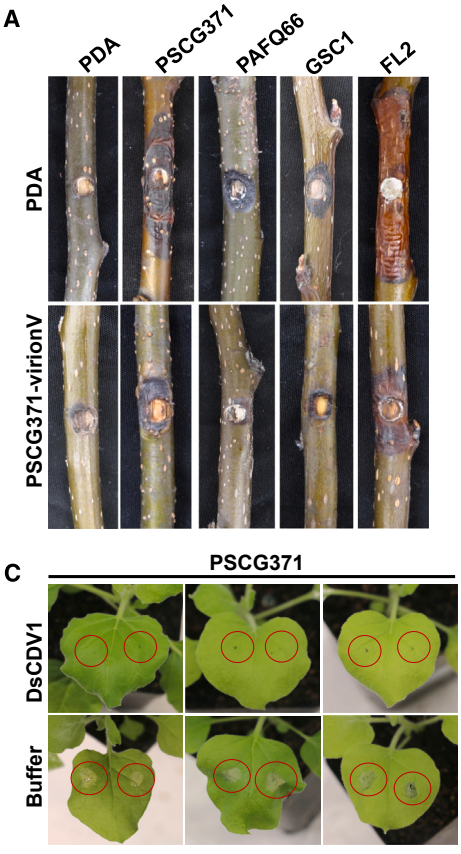

Figure 5. Effect of DsCDV1 infection on plant resistance against pathogenic fungi.

(A and B) Symptoms induced by the challenge inoculation of mycelial disks of *D. fusicola* strain PSCG371, *Colletotrichum fructicola* strain PAFQ66, *Alternaria alternata* strain GSC1, and *Valsa pyri* strain FL2 on pear (*P. pyrifolia* var. Cuiguan) shoots pre-inoculated with PDA (upper panel) or PSCG371-virionV (lower panel) at 7 dpi **(A)**, accompanied by the corresponding bar graph illustrating resultant lesion sizes **(B)**.

(C and D) Symptoms induced by the challenge inoculation mycelial disks of *D. fusicola* strain PSCG371 on *N. benthamiana* leaves pre-inoculated with purified DsCDV1 particles (upper panel) or inoculation buffer (lower panel) at 2 dpi **(C)**, accompanied by the corresponding bar graph illustrating resultant lesion sizes **(D)**. Asterisks indicate significant differences ($p < 0.05$).

purification and TEM observation. Virion particles identical to those purified from strain PSCG510 were observed, illustrating that the infectious clone successfully infects *N. benthamiana* plants (Supplemental Figure 4B).

When basal leaves of fresh *N. benthamiana* seedlings were mechanically inoculated with sap extracts of *N. benthamiana* seedlings previously inoculated with strain PSCG510 mycelia, viral particles, or the infectious clone, while apical leaves of these treated seedlings were collected and then subjected to PCR for DsCDV1 detection, 10/12, 20/22, and 28/39 plants inoculated with sap extracts of seedlings previously inoculated with PSCG510 mycelia, viral particles, or the infectious clone, respectively, were positive for DsCDV1 infection, suggesting that DsCDV1 is infectious and mechanically transmissible through plant sap (Figure 4G and Supplemental Figure 6). DsCDV1-infected seedlings of *N. benthamiana* were then grown in the greenhouse at 25°C with a 12-h photoperiod. These plants did not develop any viral symptoms (Figure 4D), suggesting that DsCDV1 can independently and systemically infect plants without causing viral disease symptoms.

DsCDV1 infection of plants confers broad-specturm resistance against diverse pathogenic fungi

To investigate whether DsCDV1 infection of pear plants confers resistance against fungal diseases, mycelial plugs of various phytopathogenic fungi, including *Diaporthe fusicola* (strain PSCG371), *Colletotrichum fructicola* (strain PAFQ66), *Alternaria alternata* (strain GSC1), and *Valsa pyri* (strain FL2), were individually used to challenge inoculate pear shoots (var. Cuiguan) pre-inoculated with either DsCDV1-infected strain PSCG371-virionV or PDA. Lesions induced by all fungal strains tested were significantly smaller at 7 dpi on pear shoots pre-inoculated with strain PSCG371-virionV as compared to those pre-inoculated with PDA (Figure 5A and 5B).

Additionally, mycelial plugs of strain PSCG371 were used to challenge inoculate apical leaves of *N. benthamiana* seedlings that were pre-inoculated with the purified DsCDV1 particles or inoculation buffer. Very small lesions, 1–5 mm in diameter, were observed on 6 out of 24 leaves pre-inoculated with the DsCDV1 particles purified. In contrast, large necrotic lesions, 7–15 mm in diameter, developed on 24 out of 24 leaves pre-inoculated with inoculation buffer (Figure 5C and 5D). These results confirm that DsCDV1 confers resistance to *N. benthamiana* against fungal diseases.

Furthermore, the *N. benthamiana* leaves used for challenge inoculation were collected and subjected to fungal isolation, resulting in 13 subisolates of strain PSCG371 as identified by their morphologies and ITS sequences. PCR identification of these subisolates revealed that five of them were positive for DsCDV1 infection (Supplemental Figure 7A). Further culture indicated these DsCDV1-infected subisolates had morphologies and growth rates similar to those of the DsCDV1-positive transfectants of PSCG371, namely PSCG371-1.5merV and -virionV (Supplemental Figure 7B and 7C). These results suggest that *D. sojae* can acquire DsCDV1 from infected plants.

DsCDV1 P3 is a movement-related protein

To identify movement-related protein(s) that allow DsCDV1 to systemically infect plants, each ORF sequence encoding P1–P4 was individually cloned into an expression vector (Figure 1E), fused with a yellow fluorescence protein (YFP) gene, transiently expressed in *N. benthamiana* leaves with or without DsCDV1 infection, and examined by confocal microscopy. In both cases (with or without DsCDV1 infection), yellow fluorescence was uniformly spread on the cellular membrane of leaf cells inoculated with the vector expressing YFP non-fused (empty vector) or fused with P1

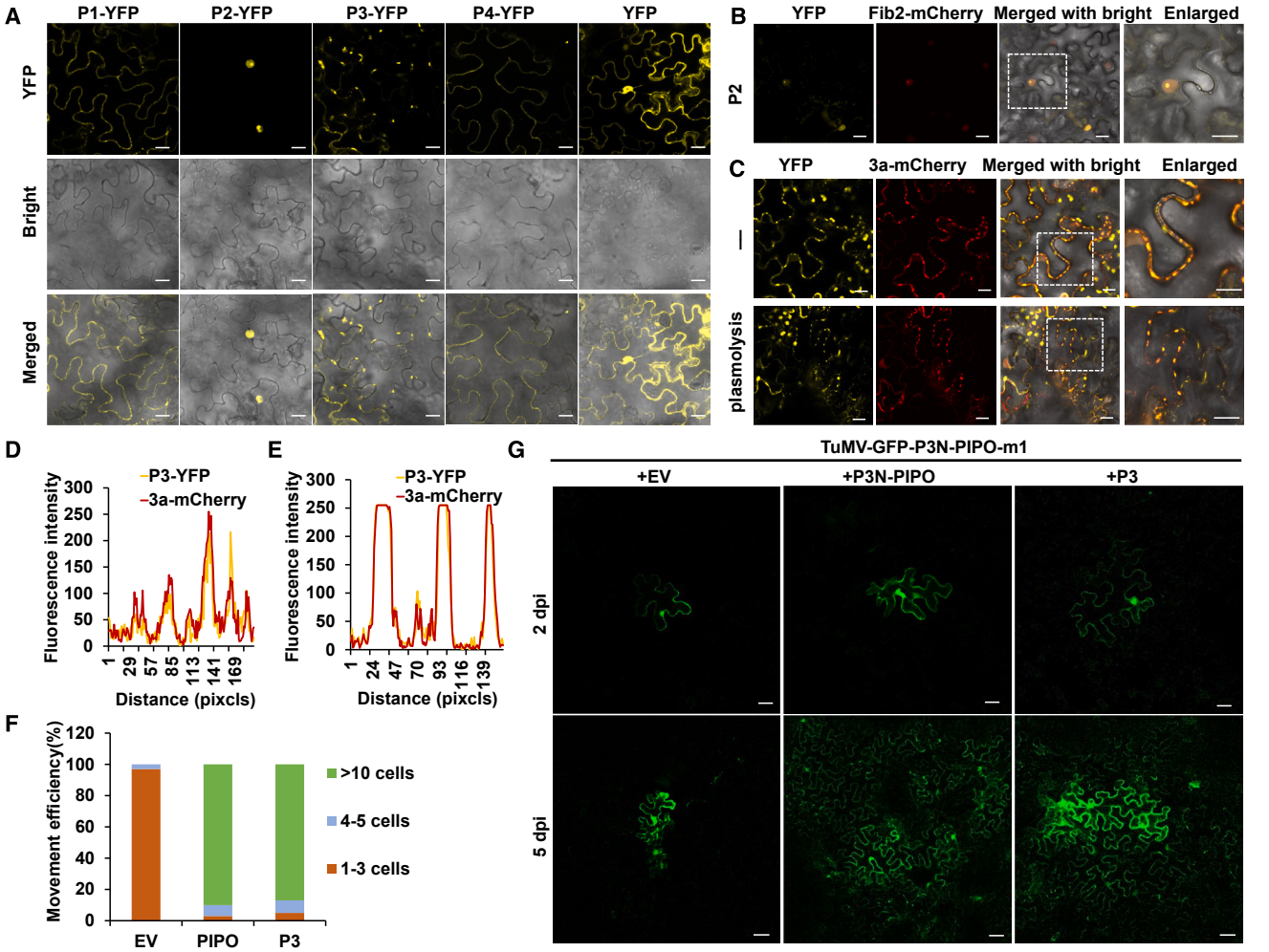

Figure 6. DsCDV1 P3 is involved in intercellular viral movement.

(A) Subcellular localization of DsCDV1 putative proteins P1-, P2-, P3-, and P4-fused YFPs, and the empty expression vector (EV) containing YFP.

(B) Subcellular localization of P2-YFP in combination with the nucleolus marker Fib2-mCherry in *N. benthamiana* leaves in the presence of DsCDV1 at 48 h post infection.

(C–E) (C) Subcellular localization of P3-YFP in combination with the PD marker 3a-mCherry in *N. benthamiana* leaves in the presence of DsCDV1 at 48 h post inoculation before (upper panel) and after (lower panel) cellular plasmolysis, accompanied by bar graphs illustrating the overlapping fluorescence spectra for P3-YFP and 3a-mCherry signals before **(D)** and after **(E)** cellular plasmolysis.

(F and G) Fluorescence diffusion patterns of the movement-deficient plant virus infectious clone TuMV-P3N-PIPO-m1 in *N. benthamiana* leaves following co-infiltration with the EV, MP P3N-PIPO, and P3 at 2 dpi (upper panel) and 5 dpi (lower panel) **(G)**, accompanied by a bar graph illustrating the proportion of fluorescent cells based on 40 images at 5 dpi **(F)**.

Scale bars, 20 μm.

and P4 (Figure 6A). However, P2-YFP was localized in the nucleolus of leaf cells, and P3-YFP was localized in plasmodesmata (PD), as confirmed respectively by the red fluorescence released by the nucleolus marker Fib2-mCherry (Figure 6B) and the PD marker 3a-mCherry (Figure 6C, upper panel). Furthermore, when 10% NaCl solution was infiltrated into *N. benthamiana* leaves to induce cellular plasmolysis, P3-YFP was still co-localized with 3a-mCherry in PD during plasmolysis (Figure 6C and 6E).

Since P3 was shown to localize in PD, similar to plant MPs (Heinlein, 2015), we hypothesized it may be an MP. To test this hypothesis, a movement-deficient infectious clone of turnip mosaic virus (TuMV-GFP-P3N-PIPO-m1) was co-infiltrated into *N. benthamiana* leaves with either the empty expression vector (EV), the P3N-PIPO vector encoding TuMV MP, or the P3-expressing vector. Forty random images from each leaf were observed under a confocal fluorescence microscope. At 2 dpi, GFP fluorescence was observed in individual cells at the inoculation sites (Figure 6G). At 5 dpi, this fluorescence quickly diffused into adjacent cells across a >10-cells radius when P3N-PIPO (90% incidence) or P3 (87%) were expressed, whereas it remained mostly restricted to the inoculation sites with very limited diffusion across a <3-cells radius for 97% of individual cells when only EV was present (Figure 6F and 6G).

DISCUSSION

The genus *Diaporthe* contains several species that infect numerous economically important crop plants worldwide,

resulting in huge losses (Diogo et al., 2010; Gomes et al., 2013; Huang et al., 2013; Gao et al., 2017; Guo et al., 2020). Screening for mycoviruses in *Diaporthe* spp. may identify viruses with the potential to be used for biological control in the future. Several RNA mycoviruses have already been identified and characterized (Preisig et al., 2000; Moleleki et al., 2003; Koloniuk et al., 2014; Zhang et al., 2015; Hrabáková et al., 2017; Xu et al., 2022), including three dsRNA viruses: Diaporthe pseudophoenicicola chrysovirus 1 (DpCV1) (Xu et al., 2022), Diaporthe ambigua RNA virus (DaRV) (Preisig et al., 2000), and Phomopsis vexans RNA virus 1 (PvRV1) (Zhang et al., 2015); two +ssRNA viruses: Phomopsis longicolla hypovirus 1 (PlHV1-ME711) (Koloniuk et al., 2014) and Phomopsis longicolla hypovirus 1 (PlRV1) (Hrabáková et al., 2017); and one −ssRNA virus: Diaporthe RNA virus (DRV1) (Moleleki et al., 2003). To our knowledge, no DNA mycoviruses have been reported in previous studies of *Diaporthe* spp. Here, we identified and characterized a novel circular ssDNA mycovirus, DsCDV1, representing the first report of a circular ssDNA mycovirus from *Diaporthe* spp.

Through a combination of HTS, PCR, and RCA approaches, the full-length genome sequence of DsCDV1 was determined and found to be a monopartite ssDNA 3185 nt in size. Searches for ORFs in the DsCDV1 genome revealed that it encodes a fused Rep and a putative CP in an ambisense orientation, a common feature among circular ssDNA viruses (Krupovic et al., 2016). The Rep of DsCDV1 contains conserved motifs, including HUH endonuclease domain (with RCR motifs I, II, and III) at the N terminus and the superfamily 3 (SF3) helicase domain (Walker-A, Walker-B, and motif C) at the C terminus, crucial for the replication of circular ssDNA viruses (Nash et al., 2011; Kazlauskas et al., 2019). The Rep and CP terminal regions contain a large IR with a conserved nona-nucleotide sequence in the stem loop, a characteristic shared with other circular ssDNA viruses and bacterial plasmids that replicate through the RCR mechanism, initiating from a conserved nona-nucleotide sequence (Heyraud-Nitschke et al., 1995; Laufs et al., 1995; Timchenko et al., 1999; Rosario et al., 2012). Despite being classified as a typical circular ssDNA mycovirus, the molecular characterization of DsCDV1 genome highlights several unique traits. (1) DsCDV1 monopartite genome 3185 nt in size is longer than those of related members in the families *Geminiviridae* (1 or 2 segments of 2.7–3.0 kb per segment) and *Genomoviridae* (1 segment with 2–2.3 kb in size for SsHADV-1; 3 segments of 1309–1320 nt for FgGMTV1; 4 segments of 1669–1770 nt for BcssDV1) (Yu et al., 2010; Li et al., 2020; Ruiz-Padilla et al., 2023). (2) DsCDV1 forms isometric particles 21–26 nm in diameter, slightly larger than those of members in the families *Geminiviridae* (twin icosahedra, 22 × 38 nm) and *Genomoviridae* (19–22 nm for SsHADV-1 and FgGMTV1) (Yu et al., 2010; Fondong, 2013; Li et al., 2020). (3) DsCDV1 has a divergent genomic organization as compared to members of the families *Geminiviridae* and *Genomoviridae*, with a Rep gene split by an IR (257 nt) and an ultra-long large IR (681 nt) (Fondong, 2013; Krupovic et al., 2016). (4) Multiple alignments of Rep sequences of DsCDV1 and related circular ssDNA viruses indicate seven conserved motifs with divergence in Motif I and Walker-A (Figure 1F). Notably, the Walker-A motif is composed of "GxxxxYKT" for DsCDV1 instead of the extremely conserved "GxxxxGKT/S" among the families *Geminiviridae* and *Genomoviridae*, a motif playing a crucial role in replication (Fondong, 2013; Krupovic et al., 2016). (5) The nona-nucleotide used for replication initiation in DsCDV1 is "TAACATTAA," differing from "TAATATTAC" and "TAATATTAT" reported in members of the families *Geminiviridae* and *Genomoviridae*, respectively.

Based on their Rep and CP sequences, DsCDV1 and two uncharacterized mycoviruses (PiCV1 and DpDV1) are phylogenetically grouped into a unique cluster distinct from related viruses in both the *Geminiviridae* and *Genomoviridae* families (Figure 2). Notably, the genome of DsCDV1 encodes for an MP, a unique feature not reported in the family *Genomoviridae* (*Ge-* for geminivirus-like, *nomo-* for no MP). These results strongly support the establishment of a new family to accommodate DsCDV1, PiCV1, and DpDV1.

Reps are widely used for identification, classification, and assessment of the diversity of circular ssDNA viruses. However, the Reps of most ssDNA viruses (71%) are chimeric proteins that exhibit incongruent evolutionary histories in their nuclease and helicase domains (Kazlauskas et al., 2018; de la Higuera et al., 2020). Such recombination events are rare among viruses of established ssDNA virus families, suggesting that the pairing of both nuclease and helicase domains in these virus groups is optimized for specific hosts/environments and that interfamilial recombinations are mostly unfavorable (Kazlauskas et al., 2018). Here, our findings reveal that the DsCDV1 Rep is a chimeric protein and is phylogenetically related to those of both established families *Geminiviridae* and *Genomoviridae* (Figure 2A). This provides strong supporting evidence that DsCDV1 represents an evolutionary link between fungal and plant circular ssDNA viruses. To date, the origins of circular ssDNA viruses infecting plants and fungi remain obscure; however, geminiviruses have been previously hypothesized to have originated from transposable elements (likely retrotransposons or helitrons) of the plants (Anirudha and Bikash, 2020). This is because plant endogenous virus-like elements contain the deconstructed Rep gene along with an IR, serving as the signature for the origin of replication in the geminivirus sense strand, and geminiviruses follow replication patterns similar to those of helitrons (Anirudha and Bikash, 2020). However, the difference in helicase domains (SF3 in place of SF1) raises the question about their evolutionary linkage (Anirudha and Bikash, 2020). Notably, DsCDV1 Rep shares considerably high identities with some fungal genomic sequences higher than with those of *Geminiviridae* and *Genomoviridae*, supporting the likelihood of a horizontal gene-transmission event between DsCDV1 and its fungal hosts during the evolutionary process. This suggests that DsCDV1 most likely originated from the fungal genome and evolved into an ssDNA virus that infects both plants and fungi. However, the reverse evolutionary route cannot be excluded.

Plants and fungi have been engaging in interactions for at least 400 million years, establishing complex mutualistic symbiotic relationships vital for the health of both partners (Rodriguez and Redman, 2008; Selosse et al., 2015; Roossinck, 2018). Many virus families that infect fungi have counterparts that infect plants, and in some instances phylogenetic analyses of these virus families suggest transmission between the plant and fungal kingdoms (Roossinck, 2018). Notably, a typical plant virus, cucumber mosaic virus (CMV), was identified in

the phytopathogenic fungus *Rhizoctonia solani* isolated from potatoes and could be mechanically transmitted to *N. benthamiana* plants (Andika et al., 2017). This implies that the transmission of plant viruses between plants and fungi is a natural occurrence (Roossinck, 2018). Two mycoviruses, Penicillium aurantiogriseum totivirus 1 (PaTV1) and Penicillium aurantiogriseum partitivirus 1 (PaPV1), have been reported to replicate in protoplasts derived from *N. benthamiana* and *N. tabacum* (Nerva et al., 2017), while their replication was limited to single-cell protoplasts but could not systemically infect whole plants (Nerva et al., 2017). Likewise, Cryphonectria hypovirus 1 (CHV1) could replicate in inoculated leaves of *N. tabacum* but did not spread systemically. However, co-inoculation with plant viruses or expression of the tobacco mosaic virus MP in transgenic plants enhanced systemic infection of plants with CHV1 (Bian et al., 2020). Despite these interactions, mycoviruses themselves were not demonstrated to infect both plants and fungi, likely due to the absence of a MP in previous reports. In our study, we demonstrate that DsCDV1 can systemically infect both fungi and plants independently (Figure 4). To further investigate the movement-related protein of DsCDV1 *in planta*, we analyzed the subcellular localization of several DsCDV1 proteins of unknown function. This analysis led to the conclusion that P3 functions as an MP, as it demonstrated the ability to be directed into PD, similar to that of plant viruses, which systemically infect plants via PD, connecting neighboring cells in plant tissues for efficient cell-to-cell movement (Lucas, 2006; Kumar et al., 2014; Huang and Heinlein, 2022). A *trans*-complementation experiment further indicates that P3 complements a movement-deficient mutant of turnip mosaic virus (TuMV-GFP-P3N-PIPO-m1) in systemic infections, confirming our conclusion (Figure 6). Therefore, DsCDV1 harbors an MP that facilitates its replication and movement in plants, distinguishing it from phylogenetically related mycoviruses belonging to the family *Genomoviridae*. To our knowledge, this is the first report of a mycovirus capable of systemic infection in plants.

In previous studies, SsHADV-1 and a dsRNA mycovirus, Pestalotiopsis theae chrysovirus 1 (PtCV1), have been shown to convert pathogenic fungi into beneficial endophytes, enhancing plant immunity (Zhang et al., 2020; Zhou et al., 2021). Additionally, Leptosphaeria biglobosa quadrivirus-1 (LbQV-1) has been found to enhance systemic resistance against *Leptosphaeria biglobosa* in oilseed rape (Shah et al., 2020). Our study reveals that DsCDV1 significantly attenuates the growth rates and virulence of its host fungus and could confer broad-spectrum resistance to plants against virulent fungal strains through hypovirulent strains, purified virions, or infection clones. Previous assumptions have proposed the use of fungal virus infections in plants as biocontrol agents (Andika et al., 2023). In line with this assumption, DsCDV1 confers high resistance to host plants against virulent fungal strains through systematic infection with purified virions or infectious clones, distinguishing it from SsHADV-1 and PtCV1. DsCDV1 represents an ecological link between fungal and plant viruses, playing a crucial role in building complex relationships between plants and fungi.

Collectively, DsCDV1 exhibits many unique molecular traits and demonstrates the ability to infect both plants and fungi, characteristics that are not observed in other circular ssDNA viruses. The phylogenetic analysis, coupled with these distinctive molecular and biological traits, places DsCDV1 in a new family, representing evolutionary and ecological links between fungal and plant ssDNA viruses. This contributes significantly to our understanding of ssDNA virus taxonomy, diversity, and evolution. Importantly, DsCDV1 not only substantially attenuates fungal virulence but also confers high resistance to the infected plants, making it a promising biocontrol agent for managing crop diseases.

METHODS

Fungal strains, plasmids, and plant materials

A total of 80 strains belonging to 10 phytopathogenic *Diaporthe* spp. (*D. caryae*, *D. citrichinensis*, *D. eres*, *D. fusicola*, *D. hongkongensis*, *D. padina*, *D. sojae*, *D. taoicola*, *D. unshiuensis*, and *D. velutina*) (Supplemental Table 1) were originally isolated from shoots of pear plants showing shoot canker symptoms, including *Pyrus bretschneideri*, *P. communis*, and *P. pyrifolia*), which were collected from 10 provinces (Fujian, Guizhou, Henan, Hubei, Jiangsu, Jiangxi, Liaoning, Shandong, Yunnan, and Zhejiang) and Chongqing municipality, China (Guo et al., 2020). All fungal strains were grown on PDA Petri dishes at 25°C, and stored on PDA slants at 4°C and a 25% glycerol solution at −80°C. The modified binary plant EV pCB301-2 × 35SMCS-HDVRZ-NOS, termed pCB301 in this study and used as the backbone for the construction of infectious clones, was kindly provided by Nanjing Agricultural University. The movement-deficient mutant of turnip mosaic virus (TuMV-GFP-P3N-PIPO-m1) was constructed and kindly provided by Institute of Plant Protection, Chinese Academy of Agricultural Sciences (Gong et al., 2022). The fungal EV pBluescript II SK(+) (P0092) was obtained from Wuhan MiaoLing Biotechnology, China. Pear seeds of *P. betulaefolia* were generously provided by the Fruit and Tea Research Institute, Hubei Academy of Agricultural Sciences. All plants were cultivated in a growth chamber under conditions of 60% relative humidity, 25°C, and a 16-h/8-h light/dark period.

Total RNA extraction, HTS, and analysis

All *Diaporthe* spp. strains were individually cultured on PDA for 7 days and then divided into eight groups, each containing 10 strains. The mycelia of all strains in each group were collected, mixed, ground into fine powder using a mortar and pestle in liquid nitrogen and subjected to total RNA extraction using TRIzol following the manufacturer's instructions (Thermo Fisher Scientific, Waltham, MA, USA). Approximately 1500 ng of total RNA from each group was subjected to HTS using the Illumina HiSeq XTen platform. Data analysis was performed as previously described (Yang et al., 2021). To verify the presence of putative mycoviruses, cDNA was synthesized from total RNA using Moloney murine leukemia virus (M-MLV) reverse transcriptase (Takara Bio, Shiga, Japan). Detection primers (Supplemental Table 2) were designed based on the assembled contigs of HTS and used for PCR amplification.

DNA extraction, amplification, and analysis

DNA was extracted with cetyltrimethylammonium bromide (CTAB)-based method following the procedures reported by Freeman et al. (1996). Abutted primers DsCDV1-All-F/R (Supplemental Table 2) were used for PCR amplification of nucleic acids. The PCR products were purified, ligated into the

pMD18-T vector (Takara Bio, Shiga, Japan), transformed into the competent cells of *Escherichia coli* strain Top10 (TransGen) according to the manufacturer's instructions, identified by PCR, and sequenced at Sangon Biotech (Shanghai, China). At least 10 independent clones were sequenced, analyzed via DNAMAN software (version 9.0; Lynnon Biosoft, Montreal, QC, Canada), and aligned using BLAST on the NCBI website (http://blast.st-va.ncbi.nlm.nih.gov/Blast.cgi). RCA was conducted on nucleic acids directly extracted from virion samples using the Illustra TempliPhi Amplification Kit (Cytiva, Marlborough, MA, USA). RCA products were digested with the restriction enzyme *Sac*I and visualized following 1% (w/v) agarose gel electrophoresis.

Purification and visualization of virus particles

Virus particles from mycelia and plant leaves were purified by sucrose density gradient centrifugation as described by (Wu et al. 2012) and (Trifonova et al. 2016), respectively. Sucrose fractions were carefully collected, loaded onto carbon-coated 230-mesh copper grids, negatively stained with 2% (w/v) uranyl acetate, and observed under a transmission electron microscope (H7650 and H-7000FA; Hitachi, Japan).

Sequence and phylogenetic analysis

Potential ORFs were deduced using DNAMAN software and the ORF finder tool on the NCBI website (http://ncbi.nlm.nih.gov/projects/gorf). Searches of sequence similarity were performed using BLAST on the NCBI website (http://blast.st-va.ncbi.nlm.nih.gov/Blast.cgi). Conserved protein domains were predicted by the NCBI conserved domain database (https://www.ncbi.nlm.nih.gov/Structure/bwrpsb/bwrpsb.cgi) (Marchler-Bauer et al., 2017). Multiple sequence alignments of amino acid sequences were performed using the Multiple Alignment using Fast Fourier Transform (MAFFT) online server (http://www.ebi.ac.uk/Tools/msa/mafft/). The resulting data were presented using GeneDoc software (version 2.7.0). The referenced sequences were retrieved from the NCBI GenBank database (www.ncbi.nlm.nih.gov/genome) (Supplemental Table 7), and the phylogenetic trees were constructed using the maximum-likelihood method as implemented by Molecular Evolutionary Genetics Analysis 7 (MEGA7; http://www.megasoftware.net/megamacBeta.php) and IQ-Tree (Nguyen et al., 2015) with a bootstrap value of 1000 replicates (Kumar et al., 2016). The amino acid sequence alignment was constructed with MAFFT and trimmed with TrimAL using the gappyout option (Capella-Gutiérrez et al., 2009). The best-fitting model was determined by ModelFinder (Kalyaanamoorthy et al., 2017).

Southern blotting

A digoxigenin-labeled DNA probe binding to DsCDV1 Rep region was synthesized with a commercial kit (Roche Diagnostics, Mannheim, Germany) using PCR products generated by primer pair Probe-F/R (Supplemental Table 2) as template. Southern blotting and hybridization analysis was conducted as previously described (Southern, 1975). In brief, a total of 40 μg of total DNAs was separated in 1% (w/v) agarose gel, transferred to positively charged nylon membranes (Millipore, Bedford, MA, USA) by capillary transfer using 20× saline–sodium citrate as a transfer buffer, and hybridized with the DNA probe at 50°C for 12 h after a pre-hybridization at the same temperature for 0.5 h. Following hybridization the membranes were washed, and the bound probe was detected using the anti-digoxigenin-AP chemiluminescent substrate CSPD according to the manufacturer's instructions (Roche Diagnostics, Rotkreuz, Switzerland). The results were visualized with a chemiluminescence detection system (Tianneng, Shanghai, China).

Attempted mycovirus elimination

Sporulation was induced in strain PSCG510 as previously described (Guo et al., 2020). For hyphal tipping, hyphal tips 3–5 mm in length were excised from the margins of strain PSCG510 cultured on 1.7% water-agar for 3 days and subcultured 10 times on fresh plates containing the same medium, resulting in 48 subisolates. Hyphal tipping was performed in combination with chemotherapy for 48 or 24 cultures of strain PSCG510 cultured on 1.7% water-agar supplemented with 50 μg/ml cycloheximide or ribavirin, respectively. Protoplasts were prepared from actively growing mycelia of strain PSCG510 as previously described (Zhang et al., 2009). The obtained protoplasts were diluted 10 times in sterile water and grown on PDA plates. Individual colonies were separated on fresh PDA plates, and their infection status was assessed.

Construction of infectious clones of DsCDV1

For the construction of the infectious clone of DsCDV1, RCA was conducted with primers *Xba*I-1m-F/*Bam*HI-1m-R harboring *Xba*I and *Bam*HI restriction sites (Supplemental Table 2) to obtain a full-length unit of DsCDV1, which was then ligated into pBluescript II SK(+) (pSK) (Stratagene) after both the insert and the vector were digested with *Xba*I and *Bam*HI and transformed into *E. coli* to produce clone pSK-1merDsCDV1. Furthermore, a half-length unit of DsCDV1 was amplified with primers *Bam*HI-0.5m-F/R harboring a *Bam*HI restriction site (Supplemental Table 2) and inserted into pSK-1mDsCDV1 after both the insert and the vector were digested with *Bam*HI to produce clone pSK-1.5merDsCDV1. The positive colonies harboring the pSK-1merDsCDV1 and pSK-1.5mer DsCDV1 clones were subjected to Sanger sequencing by Sangon Biotech (Shanghai, China) to confirm no mutations had been introduced. The infectious clone of pCB-1.5mDsCDV1 (vector pCB301-2x35S-HDVRZ-NOS-1) was constructed following the same strategy.

Virus transfection assays

Virus transfection was undertaken as previously described with minor modifications (Li et al., 2020). In brief, 200 μl of protoplasts were mixed with 30 μl (ca. 10 μg) of infectious clone plasmids or virus particles, transfected in 1.2 ml of STC buffer containing 40% (v/v) polyethylene glycol 4000, transferred to 5 ml of TB3 liquid medium containing 0.3% (w/v) yeast extract, 0.3% (w/v) casamino acids, and 20% (w/v) sucrose, and incubated for 16 h at 25°C in a shaker. The protoplasts were transferred into TB3 solid medium containing 0.7% (w/v) low-melt agarose and incubated in darkness at 25°C for 2–3 days, and their infection status was verified after subculturing three times.

Biological characterization of fungal strains

Fungal morphology, growth, and virulence were assessed as previously described (Guo et al., 2020). In brief, fungal mycelia were

grown on PDA at 25°C in darkness for 5 days. Mycelial plugs were then cut from the actively growing margins and placed in the middle of a PDA Petri dish for assessment of growth rate. The growth rate was calculated daily by measuring colony diameters for 4 days at 25°C. For the virulence assay, mycelial plugs were inoculated on the detached shoots of *P. pyrifolia* var. Cuiguan and cultured in the greenhouse at 25°C with a 12-h/12-h photoperiod. Five replicates of three independent experiments were used.

Virus transmission to fungi and plants and disease monitoring

Horizontal transmission of DsCDV1 from strain PSCG510 to other *Diaporthe* strains or species was assessed according to a previously described method (Zhou et al., 2021). In brief, following co-culture of the donor strain with the recipient strain, a mycelial agar plug from the recipient strain was placed onto a fresh PDA plate. Each pairwise co-culture experiment was repeated three times.

Fungal mycelia were mechanically inoculated onto fully expanded 8-week-old leaves of pear seedlings (*P. betulaefolia*). The inoculated leaves and new apical leaves were collected, cut into small disks, incubated on PDA for 3 days, and subjected to nucleic acid extraction and DsCDV1 detection as previously described (Smith et al., 1996; Zhou et al., 2021). The incubated leaf disks were then subjected to PCR amplification with primer pairs ITS1/ITS4 and U1/U2, listed in Supplemental Table 2.

Fungal mycelia, virions, or leaf sap were homogenized in inoculation buffer (20 mM Na_2HPO_4–NaH_2PO_4, pH 7.2) and mechanically inoculated onto fully expanded leaves at the 3-week-old stage of *N. benthamiana* pre-dusted with 400-mesh carborundum powder (Sigma-Aldrich). Recombinant plasmids of DsCDV1 infectious clones were introduced into *Agrobacterium tumefaciens* strain GV3101 by heat shock. The transformants were cultured on Luria–Bertani (LB) solid medium supplemented with antibiotics (25 μg/ml rifampicin and 50 μg/ml kanamycin) at 28°C for 2 days. The newly formed colonies were transferred into LB liquid medium with the corresponding antibiotics and grown overnight. The cultures were centrifuged at 4500 *g* for 5 min, resuspended in infiltration buffer (10 mM $MgCl_2$, 10 mM 2-(*N-morpholino)ethanesulfonic acid* [pH 5.6], and 150 μM acetosyringone) to OD_{600} = 0.8, and infiltrated into the leaf epidermis of *N. benthamiana*. Controls were infiltrated with the infiltration buffer alone.

For the challenge inoculation assays on pear plants, detached shoots of *P. pyrifolia* var. Cuiguan were pre-inoculated with mycelial plugs of strain PSCG371-virionV or PDA plugs following wounding. The plugs were removed 2 dpi and replaced with the mycelial plugs of *Diaporthe fusicola* (strain PSCG371), *Colletotrichum fructicola* (strain PAFQ66), *Alternaria alternata* (strain GSC1), or *Valsa pyri* (strain FL2). For the challenge inoculation assays on *N. benthamiana*, the purified virus particles of DsCDV1 or inoculation buffer were mechanically inoculated onto the leaf of *N. benthamiana*. After 5 dpi, apex leaves were then inoculated with mycelial plugs of strain PSCG371 following wounding by punching with a needle three times. The inoculated shoots or seedlings were cultured in the greenhouse at 25°C with 12-h/12-h photoperiod, then measured and photographed at 7 dpi. Ten to 21 biological replicates were monitored for each treatment, and the results were subjected to statistical analysis as described below.

Subcellular localization of viral proteins in *N. benthamiana*

EVs for subcellular localization were constructed as previously described (Wang et al., 2021). The CMV3a-mCherry (Ur Rehman et al., 2019) and Fib2-mCherry (GenBank: AM269909) plasmids were used as PD and nucleolus marker, respectively. All constructs were transformed into *A. tumefaciens* GV3101 (Weidi Bio) using heat shock, diluted to an OD_{600} = 0.5 in infiltration buffer, and infiltrated into *N. benthamiana* leaves individually or co-infiltrated with PD marker 3a-mCherry or pCB-1.5mDsCDV1 at a 1:1 ratio of *Agrobacterium* solution in mixture. Cellular plasmolysis was induced by infiltration of 10% NaCl solution as previously described (Feng et al., 2016). The infiltrated leaf sections were viewed at 2 dpi by a confocal laser scanning microscope (TCS-SP8; Leica Microsystems, Wetzlar, Germany) with an HC PL APO CS2 63×/1.20 water objective. The excitation laser wavelengths for GFP, YFP, and mCherry were 488, 514, and 561 nm, respectively. The emission bandwidths were 524–544 nm (for YFP) and 600–620 nm (for mCherry).

Trans-complementation of MP

The coding sequences for P3 and P3N-PIPO (GenBank: NC002509) were cloned into the PCNF3 expression vector and transformed into *A. tumefaciens* GV3101, which was diluted to an OD_{600} = 0.5, as described above. The movement-deficient mutant of TuMV (TuMV-GFP-P3N-PIPO-m1) vector was transformed into *A. tumefaciens* GV3101 and diluted to OD_{600} = 0.001 to ensure single-cell expression upon infiltration into *N. benthamiana* leaves. The solution of *A. tumefaciens* transformed with TuMV-GFP-P3N-PIPO-m1 vector was infiltrated into *N. benthamiana* leaves in combination with the solution transformed with P3-expressing vector, P3N-PIPO-expressing vector, or EV PCNF3. At 2 and 5 dpi, fluorescence was monitored using confocal laser scanning microscopy as described above, with 40 images per treatment.

Statistical analysis

Statistical analysis was performed using GraphPad Prism version 6.0 (GraphPad Software, La Jolla, CA, USA). Significant differences between the control and treatment groups were analyzed using one-way analysis of variance followed by Tukey's post hoc test. Values are shown as means ± standard deviation. Differences were considered significant when $p < 0.05$.

DATA AVAILABILITY

Sequence data supporting the findings of this study have been deposited in GenBank under the accession number PP056609 for DsCDV1.

SUPPLEMENTAL INFORMATION

Supplemental information is available at *Molecular Plant Online*.

FUNDING

This work was supported by Earmarked Fund for China Agricultural Research System (grant number CARS-28) to G.W. and W.X., and the

National Natural Science Foundation of China (grant number 32172475) to W.X.

AUTHOR CONTRIBUTIONS

G.W. and W.X. conceived the study, designed the investigation, and supervised the project. X.W. conducted most of the experiments and wrote the manuscript. Y.G. collected the fungal strains. N.H. and L.W. participated in the design of the investigation. H.D., Z.H., and M.Y. conducted biological tests. I.K.-L., K.S., R.H. A.C., and W.X. improved the English, presentation, and discussion.

ACKNOWLEDGMENTS

The authors thank Prof. Xiaorong Tao, College of Plant Protection, Nanjing Agricultural University, China, for kind contribution of the vector pCB301-2×35SMCS-HDVRZ-NOS, and Prof. Fangfang Li, Institute of Plant Protection, Chinese Academy of Agricultural Sciences, Beijing, China, for kind contribution of the vector TuMV-GFP-P3N-PIPO-m1. No conflict of interest declared.

Received: January 25, 2024
Revised: April 15, 2024
Accepted: May 9, 2024
Published: May 13, 2024

REFERENCES

Anagnostakis, S.L. (1982). Biological control of chestnut blight. Science **215**:466–471. https://doi.org/10.1126/science.215.4532.466.

Andika, I.B., Wei, S., Cao, C., Salaipeth, L., Kondo, H., and Sun, L. (2017). Phytopathogenic fungus hosts a plant virus: A naturally occurring cross-kingdom viral infection. Proc. Natl. Acad. Sci. USA **114**:12267–12272. https://doi.org/10.1073/pnas.1714916114.

Andika, I.B., Tian, M., Bian, R., Cao, X., Luo, M., Kondo, H., and Sun, L. (2023). Cross-kingdom interactions between plant and fungal viruses. Annu. Rev. Virol. **10**:119–138. https://doi.org/10.1146/annurev-virology-111821-122539.

Anirudha, C., and Bikash, M. (2020). Hypotheses of virus origin and evolutionary patterns of plant viruses. In Applied Plant Virology, L.P. Awasthi, ed. (Academic Press), pp. 779–796. https://doi.org/10.1016/B978-0-12-818654-1.00054-2.

Bai, Q., Zhai, L., Chen, X., Hong, N., Xu, W., and Wang, G. (2015). Biological and molecular characterization of five Phomopsis species associated with pear shoot canker in China. Plant Dis. **99**:1704–1712. https://doi.org/10.1094/pdis-03-15-0259-re.

Bian, R., Andika, I.B., Pang, T., Lian, Z., Wei, S., Niu, E., Wu, Y., Kondo, H., Liu, X., and Sun, L. (2020). Facilitative and synergistic interactions between fungal and plant viruses. Proc. Natl. Acad. Sci. USA **117**:3779–3788. https://doi.org/10.1073/pnas.1915996117.

Capella-Gutiérrez, S., Silla-Martínez, J.M., and Gabaldón, T. (2009). trimAl: a tool for automated alignment trimming in large-scale phylogenetic analyses. Bioinformatics **25**:1972–1973. https://doi.org/10.1093/bioinformatics/btp348.

Dayaram, A., Opong, A., Jäschke, A., Hadfield, J., Baschiera, M., Dobson, R.C.J., Offei, S.K., Shepherd, D.N., Martin, D.P., and Varsani, A. (2012). Molecular characterisation of a novel cassava associated circular ssDNA virus. Virus Res. **166**:130–135. https://doi.org/10.1016/j.virusres.2012.03.009.

de la Higuera, I., Kasun, G.W., Torrance, E.L., Pratt, A.A., Maluenda, A., Colombet, J., Bisseux, M., Ravet, V., Dayaram, A., Stainton, D., et al. (2020). Unveiling crucivirus diversity by mining metagenomic data. mBio **11**:e01410-20. https://doi.org/10.1128/mBio.01410-20.

Diogo, E.L.F., Santos, J.M., and Phillips, A.J.L. (2010). Phylogeny, morphology and pathogenicity of Diaporthe and Phomopsis species on almond in Portugal. Fungal Divers. **44**:107–115. https://doi.org/10.1007/s13225-010-0057-x.

Feng, Z., Xue, F., Xu, M., Chen, X., Zhao, W., Garcia-Murria, M.J., Mingarro, I., Liu, Y., Huang, Y., Jiang, L., et al. (2016). The ER-Membrane transport system is critical for intercellular trafficking of the NSm movement protein and Tomato spotted wilt tospovirus. PLoS Pathog. **12**:e1005443. https://doi.org/10.1371/journal.ppat.1005443.

Fondong, V.N. (2013). Geminivirus protein structure and function. Mol. Plant Pathol. **14**:635–649. https://doi.org/10.1111/mpp.12032.

Freeman, S., Katan, T., and Shabi, E. (1996). Colletotrichum gloeosporioides isolates from avocado and almond fruits with molecular and pathogenicity tests. Appl. Environ. Microbiol. **62**:1014–1020. https://doi.org/10.1128/aem.62.3.1014-1020.1996.

Gao, Y., Liu, F., Duan, W., Crous, P.W., and Cai, L. (2017). Diaporthe is paraphyletic. IMA Fungus **8**:153–187. https://doi.org/10.5598/imafungus.2017.08.01.11.

García-Arenal, F., and Zerbini, F.M. (2019). Life on the edge: geminiviruses at the interface between crops and wild plant hosts. Annu. Rev. Virol. **6**:411–433. https://doi.org/10.1146/annurev-virology-092818-015536.

Ghabrial, S.A., Castón, J.R., Jiang, D., Nibert, M.L., and Suzuki, N. (2015). 50-plus years of fungal viruses. Virology **479–480**:356–368. https://doi.org/10.1016/j.virol.2015.02.034.

Gomes, R.R., Glienke, C., Videira, S.I.R., Lombard, L., Groenewald, J.Z., and Crous, P.W. (2013). Diaporthe: a genus of endophytic, saprobic and plant pathogenic fungi. Persoonia **31**:1–41. https://doi.org/10.3767/003158513x666844.

Gong, P., Zhao, S., Liu, H., Chang, Z., Li, F., and Zhou, X. (2022). Tomato yellow leaf curl virus V3 protein traffics along microfilaments to plasmodesmata to promote virus cell-to-cell movement. Sci. China Life Sci. **65**:1046–1049. https://doi.org/10.1007/s11427-021-2063-4.

Guarnaccia, V., Groenewald, J.Z., Woodhall, J., Armengol, J., Cinelli, T., Eichmeier, A., Ezra, D., Fontaine, F., Gramaje, D., Gutierrez-Aguirregabiria, A., et al. (2018). Diaporthe diversity and pathogenicity revealed from a broad survey of grapevine diseases in Europe. Persoonia **40**:135–153. https://doi.org/10.3767/persoonia.2018.40.06.

Guo, Y.S., Crous, P.W., Bai, Q., Fu, M., Yang, M.M., Wang, X.H., Du, Y.M., Hong, N., Xu, W.X., and Wang, G.P. (2020). High diversity of Diaporthe species associated with pear shoot canker in China. Persoonia **45**:132–162. https://doi.org/10.3767/persoonia.2020.45.05.

Halary, S., Duraisamy, R., Fancello, L., Monteil-Bouchard, S., Jardot, P., Biagini, P., Gouriet, F., Raoult, D., and Desnues, C. (2016). Novel single-stranded DNA circular viruses in pericardial fluid of patient with recurrent pericarditis. Emerg. Infect. Dis. **22**:1839–1841. https://doi.org/10.3201/eid2210.160052.

Heiniger, U., and Rigling, D. (1994). Biological control of chestnut blight in Europe. Annu. Rev. Phytopathol. **32**:581–599. https://doi.org/10.1146/annurev.py.32.090194.003053.

Heinlein, M. (2015). Plant virus replication and movement. Virology **479–480**:657–671. https://doi.org/10.1016/j.virol.2015.01.025.

Heyraud-Nitschke, F., Schumacher, S., Laufs, J., Schaefer, S., Schell, J., and Gronenborn, B. (1995). Determination of the origin cleavage and joining domain of geminivirus Rep proteins. Nucleic Acids Res. **23**:910–916. https://doi.org/10.1093/nar/23.6.910.

Hillman, B.I., Annisa, A., and Suzuki, N. (2018). Viruses of plant-interacting fungi. Adv. Virus Res. **100**:99–116. https://doi.org/10.1016/bs.aivir.2017.10.003.

Hrabáková, L., Koloniuk, I., and Petrzik, K. (2017). Phomopsis longicolla RNA virus 1 – Novel virus at the edge of myco- and plant viruses. Virology **506**:14–18. https://doi.org/10.1016/j.virol.2017.03.003.

Huang, C., and Heinlein, M. (2022). Function of plasmodesmata in the interaction of plants with microbes and viruses. Methods Mol. Biol. **2457**:23–54. https://doi.org/10.1007/978-1-0716-2132-5_2.

Huang, F., Hou, X., Dewdney, M.M., Fu, Y., Chen, G., Hyde, K.D., and Li, H. (2013). Diaporthe species occurring on citrus in China. Fungal Divers. **61**:237–250. https://doi.org/10.1007/s13225-013-0245-6.

Kalyaanamoorthy, S., Minh, B.Q., Wong, T.K.F., von Haeseler, A., and Jermiin, L.S. (2017). ModelFinder: fast model selection for accurate phylogenetic estimates. Nat. Methods **14**:587–589. https://doi.org/10.1038/nmeth.4285.

Kazlauskas, D., Varsani, A., and Krupovic, M. (2018). Pervasive chimerism in the replication-associated proteins of uncultured single-stranded DNA viruses. Viruses **10**:187. https://doi.org/10.3390/v10040187.

Kazlauskas, D., Varsani, A., Koonin, E.V., and Krupovic, M. (2019). Multiple origins of prokaryotic and eukaryotic single-stranded DNA viruses from bacterial and archaeal plasmids. Nat. Commun. **10**:3425. https://doi.org/10.1038/s41467-019-11433-0.

Khalifa, M.E., and MacDiarmid, R.M. (2021). A mechanically transmitted DNA mycovirus is targeted by the defence machinery of its host, Botrytis cinerea. Viruses **13**:1315. https://doi.org/10.3390/v13071315.

Koloniuk, I., El-Habbak, M.H., Petrzik, K., and Ghabrial, S.A. (2014). Complete genome sequence of a novel hypovirus infecting Phomopsis longicolla. Arch. Virol. **159**:1861–1863. https://doi.org/10.1007/s00705-014-1992-8.

Kondo, H., Botella, L., and Suzuki, N. (2022). Mycovirus diversity and evolution revealed/inferred from recent studies. Annu. Rev. Phytopathol. **60**:307–336. https://doi.org/10.1146/annurev-phyto-021621-122122.

Kraberger, S., Schreck, J., Galilee, C., and Varsani, A. (2021). Genome sequences of microviruses identified in a sample from a sewage treatment oxidation pond. Microbiol. Resour. Announc. **10**:e00373-21–e00321. https://doi.org/10.1128/mra.00373-21.

Kraberger, S., Farkas, K., Bernardo, P., Booker, C., Argüello-Astorga, G.R., Mesléard, F., Martin, D.P., Roumagnac, P., and Varsani, A. (2015). Identification of novel Bromus- and Trifolium-associated circular DNA viruses. Arch. Virol. **160**:1303–1311. https://doi.org/10.1007/s00705-015-2358-6.

Krupovic, M. (2013). Networks of evolutionary interactions underlying the polyphyletic origin of ssDNA viruses. Curr. Opin. Virol. **3**:578–586. https://doi.org/10.1016/j.coviro.2013.06.010.

Krupovic, M., Ghabrial, S.A., Jiang, D., and Varsani, A. (2016). *Genomoviridae*: a new family of widespread single-stranded DNA viruses. Arch. Virol. **161**:2633–2643. https://doi.org/10.1007/s00705-016-2943-3.

Kumar, D., Kumar, R., Hyun, T.K., and Kim, J.-Y. (2015). Cell-to-cell movement of viruses via plasmodesmata. J. Plant Res. **128**:37–47. https://doi.org/10.1007/s10265-014-0683-6.

Kumar, S., Stecher, G., and Tamura, K. (2016). MEGA7: molecular evolutionary genetics analysis version 7.0 for bigger datasets. Mol. Biol. Evol. **33**:1870–1874. https://doi.org/10.1093/molbev/msw054.

Lal, A., Vo, T.T.B., Sanjaya, I.G.N.P.W., Ho, P.T., Kim, J.-K., Kil, E.-J., and Lee, S. (2020). Nanovirus disease complexes: An emerging threat in the modern era. Front. Plant Sci. **11**, 558403. https://doi.org/10.3389/fpls.2020.558403.

Laufs, J., Traut, W., Heyraud, F., Matzeit, V., Rogers, S.G., Schell, J., and Gronenborn, B. (1995). In vitro cleavage and joining at the viral origin of replication by the replication initiator protein of tomato yellow leaf curl virus. Proc. Natl. Acad. Sci. USA **92**:3879–3883. https://doi.org/10.1073/pnas.92.9.3879.

Li, F., Qiao, R., Wang, Z., Yang, X., and Zhou, X. (2022). Occurrence and distribution of geminiviruses in China. Sci. China Life Sci. **65**:1498–1503. https://doi.org/10.1007/s11427-022-2125-2.

Li, P., Wang, S., Zhang, L., Qiu, D., Zhou, X., and Guo, L. (2020). A tripartite ssDNA mycovirus from a plant pathogenic fungus is infectious as cloned DNA and purified virions. Sci. Adv. **6**:eaay9634. https://doi.org/10.1126/sciadv.aay9634.

Li, W., Gu, Y., Shen, Q., Yang, S., Wang, X., Wan, Y., and Zhang, W. (2015). A novel gemycircularvirus from experimental rats. Virus Gene. **51**:302–305. https://doi.org/10.1007/s11262-015-1238-1.

Lucas, W.J. (2006). Plant viral movement proteins: agents for cell-to-cell trafficking of viral genomes. Virology **344**:169–184. https://doi.org/10.1016/j.virol.2005.09.026.

Marchler-Bauer, A., Bo, Y., Han, L., He, J., Lanczycki, C.J., Lu, S., Chitsaz, F., Derbyshire, M.K., Geer, R.C., Gonzales, N.R., et al. (2017). CDD/SPARCLE: functional classification of proteins via subfamily domain architectures. Nucleic Acids Res. **45**:D200–D203. https://doi.org/10.1093/nar/gkw1129.

Marzano, S.-Y.L., Nelson, B.D., Ajayi-Oyetunde, O., Bradley, C.A., Hughes, T.J., Hartman, G.L., Eastburn, D.M., and Domier, L.L. (2016). Identification of diverse mycoviruses through metatranscriptomics characterization of the viromes of five major fungal plant pathogens. J. Virol. **90**:6846–6863. https://doi.org/10.1128/jvi.00357-16.

Moleleki, N., van Heerden, S.W., Wingfield, M.J., Wingfield, B.D., and Preisig, O. (2003). Transfection of Diaporthe perjuncta with Diaporthe RNA virus. Appl. Environ. Microbiol. **69**:3952–3956. https://doi.org/10.1128/aem.69.7.3952-3956.2003.

Mu, F., Xie, J., Cheng, S., You, M.P., Barbetti, M.J., Jia, J., Wang, Q., Cheng, J., Fu, Y., Chen, T., et al. (2017). Virome characterization of a collection of S. sclerotiorum from Australia. Front. Microbiol. **8**:2540. https://doi.org/10.3389/fmicb.2017.02540.

Nash, T.E., Dallas, M.B., Reyes, M.I., Buhrman, G.K., Ascencio-Ibañez, J.T., and Hanley-Bowdoin, L. (2011). Functional analysis of a novel motif conserved across geminivirus Rep proteins. J. Virol. **85**:1182–1192. https://doi.org/10.1128/jvi.02143-10.

Nerva, L., Varese, G.C., Falk, B.W., and Turina, M. (2017). Mycoviruses of an endophytic fungus can replicate in plant cells: evolutionary implications. Sci. Rep. **7**:1908. https://doi.org/10.1038/s41598-017-02017-3.

Nery, F.M.B., Batista, J.G., Melo, F.F.S., Ribeiro, S.G., Boiteux, L.S., Melo, F.L., Silva, J.G.I., Reis, L.d.N.A., and Pereira-Carvalho, R.C. (2023). Novel plant-associated genomoviruses from the Brazilian Cerrado biome. Arch. Virol. **168**:286. https://doi.org/10.1007/s00705-023-05892-6.

Nguyen, L.-T., Schmidt, H.A., von Haeseler, A., and Minh, B.Q. (2015). IQ-TREE: a fast and effective stochastic algorithm for estimating maximum-likelihood phylogenies. Mol. Biol. Evol. **32**:268–274. https://doi.org/10.1093/molbev/msu300.

Preisig, O., Moleleki, N., Smit, W.A., Wingfield, B.D., and Wingfield, M.J. (2000). A novel RNA mycovirus in a hypovirulent isolate of the plant pathogen Diaporthe ambigua. J. Gen. Virol. **81**:3107–3114. https://doi.org/10.1099/0022-1317-81-12-3107.

Priyashantha, A.K.H., Dai, D.-Q., Bhat, D.J., Stephenson, S.L., Promputtha, I., Kaushik, P., Tibpromma, S., and Karunarathna, S.C. (2023). Plant–fungi interactions: Where it goes? Biology **12**:809. https://doi.org/10.3390/biology12060809.

Qu, Z., Zhao, H., Zhang, H., Wang, Q., Yao, Y., Cheng, J., Lin, Y., Xie, J., Fu, Y., and Jiang, D. (2020). Bio-priming with a hypovirulent phytopathogenic fungus enhances the connection and strength of microbial interaction network in rapeseed. npj Biofilms Microbiomes **6**:45. https://doi.org/10.1038/s41522-020-00157-5.

Raco, M., Vainio, E.J., Sutela, S., Eichmeier, A., Hakalová, E., Jung, T., and Botella, L. (2022). High diversity of novel viruses in the tree pathogen Phytophthora castaneae revealed by high-throughput sequencing of total and small RNA. Front. Microbiol. **13**, 911474. https://doi.org/10.3389/fmicb.2022.911474.

Rodriguez, R., and Redman, R. (2008). More than 400 million years of evolution and some plants still can't make it on their own: plant stress tolerance via fungal symbiosis. J. Exp. Bot. **59**:1109–1114. https://doi.org/10.1093/jxb/erm342.

Rojas, M.R., Macedo, M.A., Maliano, M.R., Soto-Aguilar, M., Souza, J.O., Briddon, R.W., Kenyon, L., Rivera Bustamante, R.F., Zerbini, F.M., Adkins, S., et al. (2018). World Management of Geminiviruses. Annu. Rev. Phytopathol. **56**:637–677. https://doi.org/10.1146/annurev-phyto-080615-100327.

Roossinck, M.J. (2019). Evolutionary and ecological links between plant and fungal viruses. New Phytol. **221**:86–92. https://doi.org/10.1111/nph.15364.

Rosario, K., Duffy, S., and Breitbart, M. (2012). A field guide to eukaryotic circular single-stranded DNA viruses: insights gained from metagenomics. Arch. Virol. **157**:1851–1871. https://doi.org/10.1007/s00705-012-1391-y.

Ruiz-Padilla, A., Turina, M., and Ayllón, M.A. (2023). Molecular characterization of a tetra segmented ssDNA virus infecting Botrytis cinerea worldwide. Virol. J. **20**:306. https://doi.org/10.1186/s12985-023-02256-z.

Ruiz-Padilla, A., Rodríguez-Romero, J., Gómez-Cid, I., Pacifico, D., and Ayllón, M.A. (2021). Novel mycoviruses discovered in the mycovirome of a Necrotrophic fungus. mBio **12**, e03705-03720. https://doi.org/10.1128/mBio.03705-20.

Saad, M.F.M., Sau, A.R., Akbar, M.A., Baharum, S.N., Ramzi, A.B., Talip, N., and Bunawan, H. (2021). Construction of infectious clones of begomoviruses: strategies, techniques and applications. Biology **10**:604. https://doi.org/10.3390/biology10070604.

Santos, J.M., Vrandečić, K., Cosić, J., Duvnjak, T., and Phillips, A.J.L. (2011). Resolving the Diaporthe species occurring on soybean in Croatia. Persoonia **27**:9–19. https://doi.org/10.3767/003158511x603719.

Schmidlin, K., Sepp, T., Khalifeh, A., Smith, K., Fontenele, R.S., McGraw, K.J., and Varsani, A. (2019). Diverse genomoviruses representing eight new and one known species identified in feces and nests of house finches (Haemorhous mexicanus). Arch. Virol. **164**:2345–2350. https://doi.org/10.1007/s00705-019-04318-6.

Scholthof, K.B.G., Adkins, S., Czosnek, H., Palukaitis, P., Jacquot, E., Hohn, T., Hohn, B., Saunders, K., Candresse, T., Ahlquist, P., et al. (2011). Top 10 plant viruses in molecular plant pathology. Mol. Plant Pathol. **12**:938–954. https://doi.org/10.1111/j.1364-3703.2011.00752.x.

Selosse, M.A., Strullu-Derrien, C., Martin, F.M., Kamoun, S., and Kenrick, P. (2015). Plants, fungi and oomycetes: a 400-million year affair that shapes the biosphere. New Phytol. **206**:501–506. https://doi.org/10.1111/nph.13371.

Shah, U.A., Kotta-Loizou, I., Fitt, B.D.L., and Coutts, R.H.A. (2020). Mycovirus-induced hypervirulence of Leptosphaeria biglobosa enhances systemic acquired resistance to Leptosphaeria maculans in Brassica napus. Mol. Plant Microbe Interact. **33**:98–107. https://doi.org/10.1094/mpmi-09-19-0254-r.

Smith, H., Wingfield, M.J., Coutinho, T., and Crous, P. (1996). Sphaeropsis sapinea and Botryosphaeria dothidea endophytic in Pinus spp. and Eucalyptus spp. in South Africa. South Afr. J. Bot. **62**:86–88. https://doi.org/10.1016/s0254-6299(15)30596-2.

Son, M., Yu, J., and Kim, K.-H. (2015). Five questions about mycoviruses. PLoS Pathog. **11**, e1005172. https://doi.org/10.1371/journal.ppat.1005172.

Southern, E.M. (1975). Detection of specific sequences among DNA fragments separated by gel electrophoresis. J. Mol. Biol. **98**:503–517. https://doi.org/10.1016/S0022-2836(75)80083-0.

Thompson, S.M., Tan, Y.P., Young, A.J., Neate, S.M., Aitken, E.A.B., and Shivas, R.G. (2011). Stem cankers on sunflower (Helianthus annuus) in Australia reveal a complex of pathogenic Diaporthe (Phomopsis) species. Persoonia **27**:80–89. https://doi.org/10.3767/003158511x617110.

Tian, B., Xie, J., Fu, Y., Cheng, J., Li, B., Chen, T., Zhao, Y., Gao, Z., Yang, P., Barbetti, M.J., et al. (2020). A cosmopolitan fungal pathogen of dicots adopts an endophytic lifestyle on cereal crops and protects them from major fungal diseases. ISME J. **14**:3120–3135. https://doi.org/10.1038/s41396-020-00744-6.

Timchenko, T., de Kouchkovsky, F., Katul, L., David, C., Vetten, H.J., and Gronenborn, B. (1999). A single Rep protein initiates replication of multiple genome components of Faba bean necrotic yellows virus,a single-stranded DNA virus of plants. J. Virol. **73**:10173–10182. https://doi.org/10.1128/jvi.73.12.10173-10182.1999.

Trifonova, E.A., Nikitin, N.A., Kirpichnikov, M.P., Karpova, O.V., and Atabekov, J.G. (2016). Obtaining and characterization of spherical particles—new biogenic platforms. Moscow Univ. Biol. Sci. Bull. **70**:194–197. https://doi.org/10.3103/s0096392515040094.

Ur Rehman, A., Li, Z., Yang, Z., Waqas, M., Wang, G., Xu, W., Li, F., and Hong, N. (2019). The coat protein of Citrus yellow vein clearing virus interacts with viral movement proteins and serves as an RNA silencing suppressor. Viruses **11**:329. https://doi.org/10.3390/v11040329.

Varsani, A., and Krupovic, M. (2021). Family *Genomoviridae*: 2021 taxonomy update. Arch. Virol. **166**:2911–2926. https://doi.org/10.1007/s00705-021-05183-y.

Wang, W., Wang, X., Tu, C., Yang, M., Xiang, J., Wang, L., Hong, N., Zhai, L., and Wang, G. (2022). Novel mycoviruses discovered from a metatranscriptomics survey of the phytopathogenic Alternaria fungus. Viruses **14**:2552. https://doi.org/10.3390/v14112552.

Wang, Y., Wang, G., Bai, J., Zhang, Y., Wang, Y., Wen, S., Li, L., Yang, Z., and Hong, N. (2021). A novel Actinidia cytorhabdovirus characterized using genomic and viral protein interaction features. Mol. Plant Pathol. **22**:1271–1287. https://doi.org/10.1111/mpp.13110.

Wu, M., Jin, F., Zhang, J., Yang, L., Jiang, D., and Li, G. (2012). Characterization of a novel bipartite double-stranded RNA mycovirus conferring hypovirulence in the phytopathogenic fungus Botrytis porri. J. Virol. **86**:6605–6619. https://doi.org/10.1128/jvi.00292-12.

Xie, J., and Jiang, D. (2014). New insights into mycoviruses and exploration for the biological control of crop fungal diseases. Annu. Rev. Phytopathol. **52**:45–68. https://doi.org/10.1146/annurev-phyto-102313-050222.

Xu, G., Zhang, X., Liang, X., Chen, D., Xie, C., Kang, Z., and Zheng, L. (2022). A novel hexa-segmented dsRNA mycovirus confers hypovirulence in the phytopathogenic fungus Diaporthe pseudophoenicicola. Environ. Microbiol. **24**:4274–4284. https://doi.org/10.1111/1462-2920.15963.

Yang, M., Xu, W., Zhou, X., Yang, Z., Wang, Y., Xiao, F., Guo, Y., Hong, N., and Wang, G. (2021). Discovery and characterization of a novel bipartite botrexvirus from the phytopathogenic fungus Botryosphaeria dothidea. Front. Microbiol. **12**, 696125. https://doi.org/10.3389/fmicb.2021.696125.

Yu, X., Li, B., Fu, Y., Xie, J., Cheng, J., Ghabrial, S.A., Li, G., Yi, X., and Jiang, D. (2013). Extracellular transmission of a DNA mycovirus and its use as a natural fungicide. Proc. Natl. Acad. Sci. USA **110**:1452–1457. https://doi.org/10.1073/pnas.1213755110.

Yu, X., Li, B., Fu, Y., Jiang, D., Ghabrial, S.A., Li, G., Peng, Y., Xie, J., Cheng, J., Huang, J., and Yi, X. (2010). A geminivirus-related DNA

mycovirus that confers hypovirulence to a plant pathogenic fungus. Proc. Natl. Acad. Sci. USA **107**:8387–8392. https://doi.org/10.1073/pnas.0913535107.

Zhang, H., Xie, J., Fu, Y., Cheng, J., Qu, Z., Zhao, Z., Cheng, S., Chen, T., Li, B., Wang, Q., et al. (2020). A 2-kb mycovirus converts a pathogenic fungus into a beneficial endophyte for brassica protection and yield enhancement. Mol. Plant **13**:1420–1433. https://doi.org/10.1016/j.molp.2020.08.016.

Zhang, L., Fu, Y., Xie, J., Jiang, D., Li, G., and Yi, X. (2009). A novel virus that infecting hypovirulent strain XG36-1 of plant fungal pathogen Sclerotinia sclerotiorum. Virol. J. **6**:96. https://doi.org/10.1186/1743-422x-6-96.

Zhang, L., Wang, S., Ruan, S., Nzabanita, C., Wang, Y., and Guo, L. (2023). A mycovirus VIGS vector confers hypovirulence to a plant pathogenic fungus to control wheat FHB. Adv. Sci. **10**, e2302606. https://doi.org/10.1002/advs.202302606.

Zhang, R.J., Zhong, J., Shang, H.H., Pan, X.T., Zhu, H.J., and Gao, B.D. (2015). The complete nucleotide sequence and genomic organization of a novel victorivirus with two non-overlapping ORFs, identified in the plant-pathogenic fungus Phomopsis vexans. Arch. Virol. **160**:1805–1809. https://doi.org/10.1007/s00705-015-2420-4.

Zhao, L., Rosario, K., Breitbart, M., and Duffy, S. (2019). Eukaryotic circular Rep-encoding single-stranded DNA (CRESS DNA) viruses: ubiquitous viruses with small genomes and a diverse host range. Adv. Virus Res. **103**:71–133. https://doi.org/10.1016/bs.aivir.2018.10.001.

Zhao, X., Li, K., Zheng, S., Yang, J., Chen, C., Zheng, X., Wang, Y., and Ye, W. (2022). Diaporthe diversity and pathogenicity revealed from a broad survey of soybean stem blight in China. Plant Dis. **106**:2892–2903. https://doi.org/10.1094/pdis-12-21-2785-re.

Zhong, J., Li, P., Gao, B.D., Zhong, S.Y., Li, X.G., Hu, Z., and Zhu, J.Z. (2022). Novel and diverse mycoviruses co-infecting a single strain of the phytopathogenic fungus Alternaria dianthicola. Front. Cell. Infect. Microbiol. **12**, 980970. https://doi.org/10.3389/fcimb.2022.980970.

Zhou, L., Li, X., Kotta-Loizou, I., Dong, K., Li, S., Ni, D., Hong, N., Wang, G., and Xu, W. (2021). A mycovirus modulates the endophytic and pathogenic traits of a plant associated fungus. ISME J. **15**:1893–1906. https://doi.org/10.1038/s41396-021-00892-3.